Interfaces and Free Boundaries **19** (2017), 1–30
DOI 10.4171/IFB/375

Finite horizon model predictive control of electrowetting on dielectric with pinning

HARBIR ANTIL
Department of Mathematical Sciences, George Mason University, 4400 University Drive, Fairfax, Virginia 22030, USA
E-mail: hantil@gmu.edu

MICHAEL HINTERMÜLLER
Weierstraß-Institut, Mohrenstraße 39, 10117 Berlin, Germany
E-mail: michael.hintermueller@wias-berlin.de

RICARDO H. NOCHETTO
Department of Mathematics and Institute for Physical Science and Technology, University of Maryland, College Park MD 20742, USA
E-mail: rhn@math.umd.edu

THOMAS M. SUROWIEC
Philipps-Universität Marburg, Fachbereich Mathematik und Informatik, Hans-Meerwein-Straße 6, 35032 Marburg, Germany
E-mail: surowiec@mathematik.uni-marburg.de

DONAT WEGNER
Institut für Mathematik, Humboldt-Universität zu Berlin, Unter den Linden 6, 10099 Berlin, Germany
E-mail: dwegner@mathematik.hu-berlin.de

[Received 3 August 2015 and in revised form 11 October 2016]

A time-discrete spatially-continuous electrowetting on dielectric (EWOD) model with contact line pinning is considered as the state system in an optimal control framework. The pinning model is based on a complementarity condition. In addition to the physical variables describing velocity, pressure, and voltage, the solid-liquid-air interface, i.e., the contact line, arises as a geometric variable that evolves in time. Due to the complementarity condition, the resulting optimal control of a free boundary problem is thus a mathematical program with equilibrium constraints (MPEC) in function space. In order to cope with the geometric variable, a finite horizon model predictive control approach is proposed. Dual stationarity conditions are derived by applying a regularization procedure, exploiting techniques from PDE-constrained optimization, and then passing to the limit in the regularization parameters. Moreover, a function-space-based numerical procedure is developed by following the theoretical limit argument used in the derivation of the dual stationarity conditions. The performance of the algorithm is demonstrated by several examples; including barycenter matching and trajectory tracking.

2010 Mathematics Subject Classification: Primary 49J20, 35Q93, 35Q35, 35R35, 90C33, 90C46, 76D45, 65K10, 65K15.

Keywords: Electrowetting on dielectric, EWOD, contact line pinning, surface tension, sharp

interface, optimal control of free boundary problems, mathematical program with equilibrium constraints, MPEC, PDE-constrained optimization, barycenter matching, trajectory tracking.

1. Introduction

In this paper, we consider the control of a single droplet on an electrowetting on dielectric (EWOD) device. Electrowetting is an important technique used in the manipulation of fluids on the micro-scale in digital microfluidic devices. A typical micro-device driven by EWOD consists of two narrowly separated parallel plates in which one of the plates contains an embedded grid of electrodes. The contact angle of a droplet placed between the plates can be actuated by applying voltages to the electrodes on the grid, see, e.g., [9, 46]. Some applications include mass spectrometry [52], lab-on-a-chip [18, 45], and electrofluidic displays [20].

Building upon the developments in [48, 51], we consider as our state system (forward problem) the following time-discrete spatially-continuous EWOD model with contact line pinning (here in strong form):

$$\alpha \frac{\mathbf{u}^{i+1} - \mathbf{u}^i}{\delta t_{i+1}} + \beta \mathbf{u}^{i+1} + \nabla p^{i+1} = 0 \quad \text{in } \Omega^i, \tag{1.1a}$$

$$\operatorname{div} \mathbf{u}^{i+1} = 0 \quad \text{in } \Omega^i, \tag{1.1b}$$

$$p^{i+1}\boldsymbol{\nu}^i - \kappa^{i+1}\boldsymbol{\nu}^i - E^i\boldsymbol{\nu}^i - \lambda^{i+1}\boldsymbol{\nu}^i - D_{\text{visc}}(\mathbf{u}^{i+1}\cdot\boldsymbol{\nu}^i)\boldsymbol{\nu}^i = 0 \quad \text{on } \Gamma^i, \tag{1.1c}$$

$$\lambda^{i+1} - P_{\text{pin}}\partial\left(||\cdot||_{L^1(\Gamma^i)}\right)(\mathbf{u}^{i+1}\cdot\boldsymbol{\nu}^i) \ni 0 \quad \text{on } \Gamma^i. \tag{1.1d}$$

Here, the time interval is partitioned into intervals of length $\delta t_i > 0$, for $i = 1, \ldots, T$; and $\Omega^i \subset \mathbb{R}^2$ and $\Gamma^i := \partial\Omega^i$ are the droplet domain and its interface at time t_i, respectively, which are always assumed to be known at t_i and sufficiently smooth. The constants $\alpha << \beta$ are non-dimensional material and geometry constants associated with the underlying device and D_{visc}, $P_{\text{pin}} > 0$ are contact-line friction coefficients.

In this model, (1.1a) represents the conservation of momentum and (1.1b) is the conservation of mass. The equation (1.1c), referred to in [51] as the "pressure boundary condition", models the effect that curvature, the electrowetting forcing term E (eventually the control), the pinning variable λ, and viscosity have on the pressure inside the droplet. Equation (1.1d) models "contact line pinning." Pinning is a naturally occurring phenomenon in many wetting applications, which is due to molecular adhesion at the solid-liquid-air interface of the droplet and contact angle hysteresis. This phenomenon ultimately slows the motion of the droplet. More specifically, a certain resistance threshold must be overcome in order for the droplet to move. The form in (1.1d) was suggested in [48, 51] as a means of approximating the computationally expensive molecular dynamics simulations suggested by the physics. Without the pinning condition (1.1d), numerical simulations of the droplets predict motions that are up to ten times faster than observed in the laboratory, cf. the discussion in [51] and the references therein. Note that due to [43, Theorem 21] (rules of generalized differentiation) the suddifferential inclusion in (1.1d) is equivalent to the pinning condition in [48, 51]. In particular, we have for any $\lambda \in P_{\text{pin}}\partial(\|\cdot\|_{L^1(\Gamma^i)})(\mathbf{u}\cdot\boldsymbol{\nu})$ the relations

$$\lambda(s) = P_{\text{pin}}\operatorname{sign}\big((\mathbf{u}\cdot\boldsymbol{\nu})(s)\big), \quad \text{for almost every (a.e.) } s \in \Gamma^i : (\mathbf{u}\cdot\boldsymbol{\nu})(s) \neq 0,$$
$$\lambda(s) \in [-P_{\text{pin}}, P_{\text{pin}}], \quad \text{for a.e. } s \in \Gamma^i : (\mathbf{u}\cdot\boldsymbol{\nu})(s) = 0.$$

Letting $\ell^+ := \max(0, \mathbf{u}\cdot\boldsymbol{\nu})$ and $\ell^- := \min(0, \mathbf{u}\cdot\boldsymbol{\nu})$, where $\max(0,\cdot)$ and $\min(0,\cdot)$ are understood in the pointwise almost everywhere sense, we derive from this the complementarity relations

$$0 \leqslant \ell^+, \quad \lambda \leqslant P_{\text{pin}}, \quad \ell^+(\lambda - P_{\text{pin}}) = 0, \qquad \text{for a.e. } s \in \Gamma^i, \tag{1.3a}$$

$$0 \geqslant \ell^-, \quad \lambda \geqslant -P_{\text{pin}}, \quad \ell^-(\lambda + P_{\text{pin}}) = 0, \qquad \text{for a.e. } s \in \Gamma^i. \tag{1.3b}$$

Given the known quantities $\mathbf{u}^i$, $\boldsymbol{\nu}^i$, E^i, and an approximation of the curvature κ^{i+1}; the velocity $\mathbf{u}^{i+1}$, pressure p^{i+1}, and pinning variable λ^{i+1} at time t_{i+1} are to be obtained by solving (1.1). Afterwards, the geometric variable Γ_i needs to be evolved.

For some $(n-1)$-dimensional manifold Γ, a positive scalar $\tau > 0$, and a vector field $\mathbf{u} : \Gamma \to \mathbb{R}^n$, we define the mapping $\mathbf{X}(\tau;\mathbf{u})(\cdot) : \Gamma \to \mathbb{R}^n$ by

$$\mathbf{X}(\tau;\mathbf{u})(\Gamma) = \Gamma + \tau\mathbf{u}(\Gamma),$$

where '+' is understood in the sense that for $x \in \Gamma$, $\mathbf{X}(\tau;\mathbf{u})(x) = x + \tau\mathbf{u}(x)$. Clearly, $\mathbf{X}(0,\mathbf{u})(\Gamma) = \Gamma$.

Returning to the EWOD problem, we now use the velocity $\mathbf{u}^{i+1}$ (defined on Γ^i) at time t_{i+1} along with $\mathbf{X}$ to update the boundary Γ^i and approximate curvature term κ^{i+1}. For simplicity, we write $\mathbf{X}^{i+1}(\delta t_{i+1}) := \mathbf{X}(\delta t_{i+1};\mathbf{u}^{i+1})$. Note that $\mathbf{X}^{i+1}(0)$ is the identity mapping on Γ^i. We then set

$$\Gamma^{i+1} := \mathbf{X}^{i+1}(\delta t_{i+1})(\Gamma^i) \text{ and } \kappa^{i+1}\cdot\boldsymbol{\nu}^i(\cdot) := -\Delta_{\Gamma^i}\mathbf{X}^{i+1}(0)(\cdot) - \delta t_{i+1}\Delta_{\Gamma^i}\mathbf{u}^{i+1}(\cdot). \tag{1.4}$$

Here, Δ_{Γ^i} denotes the Laplace-Beltrami operator on Γ^i; see e.g., [13].

Ideally one would like to (simultaneously) control the EWOD system (1.1) over all time periods, through a suitable choice of E^i for each i that minimizes some objective $\mathfrak{J}$. Then, by letting

$$\mathbf{E} := (E^1,\dots,E^T),\ \mathbf{Z} := \big((\mathbf{u}^1,\dots,\mathbf{u}^T),(p^1,\dots,p^T),(\lambda^1,\dots,\lambda^T)\big),\ \boldsymbol{\Gamma} := (\Gamma^1,\dots,\Gamma^T),$$

this would require the solution to an optimal control problem of the following form:

$$\begin{aligned}
&\min\ \mathfrak{J}(\mathbf{E},\mathbf{Z},\boldsymbol{\Gamma}) \text{ over } (\mathbf{E},\mathbf{Z},\boldsymbol{\Gamma}) \in \mathfrak{X}\\
&\text{subject to (s.t.)} \forall i = 1,\dots,N:\\
&\qquad \alpha\frac{\mathbf{u}^{i+1}-\mathbf{u}^i}{\delta t_{i+1}} + \beta\mathbf{u}^{i+1} + \nabla p^{i+1} = 0 \quad \text{in } \Omega^i,\\
&\qquad \operatorname{div}\mathbf{u}^{i+1} = 0 \quad \text{in } \Omega^i,\\
&\qquad p^{i+1}\boldsymbol{\nu}^i - \kappa^{i+1}\boldsymbol{\nu}^i - E^i\boldsymbol{\nu}^i - \lambda^{i+1}\boldsymbol{\nu}^i - D_{\text{visc}}(\mathbf{u}^{i+1}\cdot\boldsymbol{\nu}^i)\boldsymbol{\nu}^i = 0 \quad \text{on } \Gamma^i,\\
&\qquad \lambda^{i+1} - P_{\text{pin}}\partial\left(||\cdot||_{L^1(\Gamma^i)}\right)(\mathbf{u}^{i+1}\cdot\boldsymbol{\nu}^i) \ni 0 \quad \text{on } \Gamma^i,\\
&\qquad \Gamma^{i+1} - \mathbf{X}^{i+1}(\delta t_{i+1})(\Gamma^i) = 0,\\
&\qquad \kappa^{i+1}\cdot\boldsymbol{\nu}^i + \Delta_{\Gamma^i}\mathbf{X}^{i+1}(0) + \delta t_{i+1}\Delta_{\Gamma^i}\mathbf{u}^{i+1}, = 0\\
&\qquad E^i \in \mathfrak{E}^i_{ad}.
\end{aligned}$$

Here, $\mathfrak{E}^i_{ad}$, $i = 1,\dots,T$, represent the constraints on the controls E^i. Note, in particular, the inclusion of the definitions in (1.4) as constraints in the control problem; $\mathfrak{X}$ represents the (yet to be determined) space of decision variables.

Unfortunately, the dependencies of the operators, the underlying spaces, and the solutions on the interfaces make proving the existence of an optimal control $\mathbf{E}$ very challenging without further restrictive assumptions or additional constraints. Furthermore, from a numerical standpoint, this comprehensive constraint system would imply substantial computational effort, assuming the problem is even tractable. For this reason, we choose to pursue a more tractable approach inspired by *finite horizon* model predictive control, see, e.g., [16]; in particular we refer to the formal discussion/definition on pp. 337–338. In the context of optimal control of instationary Navier-Stokes, this has also been called "instantaneous control," see [33].

In order to describe the basic idea behind model predictive control in the current setting, we denote the control space at time t_i by $\mathfrak{E}^i$; the remaining variables $z = (\mathbf{u}, p, \lambda)$ lie in the space $\mathfrak{Z}^i$. Assuming a compatible objective function and sufficiently smooth boundaries Γ^i, we have the following model predictive control scheme.

Finite horizon model predictive control of EWOD

At time t_i we are given:

1. Ω^i, Γ^i, $\boldsymbol{\nu}^i$, δt_{i+1}, $\mathbf{u}^i$.
2. The previous control E^i and control constraints $\mathfrak{E}^i_{ad} \subset \mathfrak{E}^i$.
3. An objective $\mathfrak{J}^i(E, z)$.

Consider the minimization problem

$$\min \mathfrak{J}^i(E, z) \text{ over } (E, z) \times \mathfrak{E}^i_{ad} \times \mathfrak{Z}^i \ : \ (E, z) \text{ satisfies (1.1)}. \tag{P}$$

Assuming $E^i \in \mathfrak{E}^i_{ad}$:

1. Solve (1.1) to obtain a solution-tuple $z' := (\mathbf{u}', p', \lambda')$.
2. Find a descent direction $(\delta E, \delta z)$ that sufficiently decreases a merit function related to $\mathfrak{J}^{i+1}$ and the feasible set.
3. Update the control E^i and obtain a new solution-tuple z'.

At this point, we either repeat the process or evolve the boundary Γ^i according to the new velocity field via (1.4) and proceed to the next time step.

Although the control strategy of EWOD, as proposed above, removes some of the difficulties associated with the geometric variable Γ^i, the optimal control of a type of Darcy or Hele-Show flow coupled with a non-smooth equilibrium condition is a challenging problem in its own right. Indeed, the presence of the subdifferential inclusion (1.1d) means that we are still tasked with solving (or at least reducing the objective of) a mathematical program with equilibrium constraints (MPEC) in function space; a problem class with a notoriously degenerate constraint set, see, e.g., [11, 21, 22, 24, 29]. The constraint degeneracy here is due to the pinning condition. As a consequence, the standard methods of PDE-constrained optimization or non-linear programming in Banach spaces are not directly applicable for deriving stationarity conditions of such control problems. Moreover, the numerical solution represents a significant challenge due to the structure of the feasible set. Therefore, we need to develop the theory and numerics for one time step before passing to the evolution in time.

The influential experimental studies by C.-J. Kim et al., e.g., [8, 9, 18, 46, 52] demonstrate that one can create, split, merge, and move droplets in a laboratory setting. This led to the development

of several mathematical models (see discussion below). Thus, our paper aims to make this procedure mathematically rigorous and to find optimal switching patterns for these four essential actions of an EWOD device. To this end, we start by noting that the (suboptimal) control of a geometric partial differential equation (PDE) coupled with an equilibrium or complementarity condition (such as the pinning constraint in our context) has, to the best of our knowledge, not yet been investigated in the literature. In the context of shape optimization of super-hydrophobic/hydrophilic materials, a similar forward problem arises when using a threshold-type slip-boundary condition, see the recent paper [19]. Concerning the control of free boundaries, we mention here [4, 44], where the free boundary is implicitly treated, and [1, 2, 12, 34, 35], where the free boundary is treated in graph form. A shape optimization perspective to (geometric) complementarity problems has been investigated in [27, 28, 30]. Recently, a parameter-identification problem in the study of cell motility with both sharp and diffuse interface formulations was considered in [10] and droplet footprint control via surface tension in [38]. We would also like to mention [40], in which shape sensitivity analysis and control for time-dependent shapes with PDE-constraints is considered. Finally, we note that our techniques for the investigation of (P) are based on several approaches found in the optimal control of elliptic variational inequalities, i.e., MPECs in function space. In particular, we mention the monograph by Barbu [4] for regularization approaches and [23, 24] for efficient numerical methods and relevant stationarity concepts.

Concerning developments in the literature that are directly related to this paper, we mention, in particular, the papers [49, 50]. In [49] a droplet model, based on [50], is considered in the context of model-predictive/open-loop control. More specifically, the actuation of particles within droplets is considered. Though the model is largely phenomenological, the results are very convincing and have clearly impacted the further studies, e.g., [51]. In both our paper as well as [48–51], topological changes can only be handled heuristically as the pressure boundary condition contains a curvature term that becomes undefined once droplets pinch-off or merge. Thus, we chose our objective functionals for examples in which topology changes are not expected, e.g., tracking the barycenter of a droplet along a diagonal and tracking an ideal droplet's trajectory. Since we are in a time-discrete setting, it seems possible to also allow topological changes by using the heuristic mentioned above to split or merge between the calculation of controls E^i and E^{i+1}.

The rest of the paper is structured as follows. In Section 2, we introduce the necessary notation, function spaces and a distributional form of the EWOD problem (1.1). We discuss the mathematical difficulties introduced by the pinning condition and then formulate the control problems to be considered at each step of the control process described above. In Section 3 we present a limiting regularization approach that serves two purposes:

1. To determine optimality/stationarity conditions of the control problems in each time interval and
2. to provide us with a means of obtaining descent directions for the reduced objective functionals, as will be needed in the numerical scheme.

The dual multiplier-based stationarity conditions are reminiscent of the limiting forms of C-stationarity, which are common in the literature, see e.g., [24, 29, 32]. In Section 4, we discuss all the details surrounding the numerical method and provide the results of several examples. In particular, we introduce the objective functionals for barycenter matching and barycenter tracking. Moreover, the discretization of the underlying spaces, the means of solving the (regularized) EWOD problem, and the calculation of gradients are explained. Finally, several examples are given, in which the constraint degeneracy of the underlying problem can be seen during the majority of the time steps.

2. Mathematical framework for a single time step

In this section, we provide the basic definitions and notations used throughout the text. Moreover, we define the optimization problems considered in each time step of the procedure.

2.1 *The EWOD model: Weak form*

We start by introducing the relevant notation and function spaces. Given an (open bounded) droplet domain Ω^i with smooth boundary Γ^i, we let $\mathbb{V}^i$, the "velocity space", be the closure of $C^\infty(\overline{\Omega}^i;\mathbb{R}^n)$ with respect to the norm

$$\|\mathbf{v}\|_{\mathbb{V}^i} := \left(||\mathbf{v}||^2_{H(\mathrm{div};\Omega^i)} + \delta t_i ||\nabla_{\Gamma^i}\mathbf{v}||^2_{L^2(\Gamma^i;\mathbb{R}^n)}\right)^{\frac{1}{2}}.$$

Moreover, we let E^i_{ad} be a non-empty, closed, convex subset of $E^i := L^2(\Gamma^i)$. Note, we could also take other control spaces $\mathcal{E}^i$ here, e.g., $\mathbb{R}^n$ or any other reflexive Banach space. In this context, we define the bounded linear operators $A^i : \mathbb{V}^i \to {\mathbb{V}^i}^*$, $B^i : \mathbb{V}^i \to L^2(\Omega^i)$, $C^i : \mathbb{V}^i \to L^2(\Gamma^i)$, $F^i_0 : E^i \to {\mathbb{V}^i}^*$ and the continuous affine mapping $F^i : E^i \to {\mathbb{V}^i}^*$ by

$$\begin{aligned}
\langle A^i\mathbf{u},\mathbf{v}\rangle &:= \left(\frac{\alpha}{\delta t_{i+1}} + \beta\right)\left[(\mathbf{u},\mathbf{v})_{L^2(\Omega^i;\mathbb{R}^n)} + \gamma(\mathrm{div}\,\mathbf{u},\mathrm{div}\,\mathbf{v})_{L^2(\Omega^i;\mathbb{R}^n)}\right] \\
&\quad + D_{visc}(\mathbf{u}\cdot\boldsymbol{\nu}^i,\mathbf{v}\cdot\boldsymbol{\nu}^i)_{L^2(\Gamma^i)} + \delta t_{i+1}(\nabla_{\Gamma^i}\mathbf{u},\nabla_{\Gamma^i}\mathbf{v})_{L^2(\Gamma^i;\mathbb{R}^n)}, \quad \gamma > 0, \\
\langle B^i\mathbf{u}, w\rangle &:= (-\mathrm{div}\,\mathbf{u}, w)_{L^2(\Omega^i)}, \\
\langle C^i\mathbf{u},\mu\rangle &:= (\mathbf{u}\cdot\boldsymbol{\nu}^i,\mu)_{L^2(\Gamma^i)}, \\
\langle F^i_0(E^i),\mathbf{v}\rangle &:= -(E^i,\mathbf{v}\cdot\boldsymbol{\nu}^i)_{L^2(\Gamma^i)}, \\
\langle F^i(E^i),\mathbf{v}\rangle &:= \frac{\alpha}{\delta t_{i+1}}(\mathbf{u}^i,\mathbf{v})_{L^2(\Omega^i;\mathbb{R}^n)} + \langle F^i_0(E^i),\mathbf{v}\rangle - (\nabla_{\Gamma^i}\mathbf{X}^{i+1}(0),\nabla_{\Gamma^i}\mathbf{v})_{L^2(\Gamma^i;\mathbb{R}^n)}.
\end{aligned}$$

Here, the definitions of $\langle\cdot,\cdot\rangle$ and the test functions should be clear in context. For the sake of readability, we henceforth leave off the superscripts i. Note that $\gamma > 0$ ensures the ellipticity of A on $\mathbb{V}$. Of course, for $\mathbf{u} \in \mathbb{V}$ such that $\mathrm{div}\,\mathbf{u} = 0$, this term disappears.

Using these operators and function spaces, we now state the distributional form of (1.1):

$$A\mathbf{u} + B^*p + C^*\lambda = F(E), \quad \text{in } \mathbb{V}^*, \tag{2.1a}$$

$$B\mathbf{u} = 0, \quad \text{in } L^2(\Omega), \tag{2.1b}$$

$$\lambda - P_{\mathrm{pin}}\partial\left(||\cdot||_{L^1(\Gamma)}\right)(C\mathbf{u}) \ni 0, \quad \text{in } L^2(\Gamma). \tag{2.1c}$$

Note that F_0 may also be nonlinear and smooth. This assumption on the control action would allow us to alternatively model the way in which the EWOD device delivers charges to the droplet. Although this would add a nonlinearity to the control process, it would not remove the major complications due to the complementarity, i.e., pinning, constraint. Hence, we keep F_0 simple in order to emphasize the difficulty due to the constraint degeneracy.

In the following, we briefly discuss the aforementioned degeneracy of the EWOD system as a forward problem and introduce the notion of "biactivity." In light of (1.3), the subdifferential condition (2.1c) is equivalent to

$$C\mathbf{u} - (C\mathbf{u} + \lambda - P_{\mathrm{pin}})_+ + \left(-(C\mathbf{u} + \lambda + P_{\mathrm{pin}})\right)_+ = 0, \text{ a.e. } \Gamma,$$

where "a.e." refers to "almost everywhere" and $(\cdot)_+$ signifies the superposition operator from $L^2(\Gamma) \to L^2(\Gamma)$ defined by the real-valued function $\max(0,\cdot) : \mathbb{R} \to \mathbb{R}$, i.e. the pointwise $\max(0,\cdot)$ operation on Γ. Given a pair $(\mathbf{u},\lambda)$ that satisfies (2.1c), we define the "strongly active sets" $\mathfrak{A}^+, \mathfrak{A}^- \subset \Gamma$ and the "weakly active/biactive sets" $\mathfrak{B}^+, \mathfrak{B}^- \subset \Gamma$ by

$$\begin{aligned}
\mathfrak{A}^+ &:= \left\{ s \in \Gamma \,\middle|\, \lambda(s) = P_{\text{pin}},\ (C\mathbf{u})(s) > 0 \right\},\\
\mathfrak{B}^+ &:= \left\{ s \in \Gamma \,\middle|\, \lambda(s) = P_{\text{pin}},\ (C\mathbf{u})(s) = 0 \right\},\\
\mathfrak{A}^- &:= \left\{ s \in \Gamma \,\middle|\, \lambda(s) = -P_{\text{pin}},\ (C\mathbf{u})(s) < 0 \right\},\\
\mathfrak{B}^- &:= \left\{ s \in \Gamma \,\middle|\, \lambda(s) = -P_{\text{pin}},\ (C\mathbf{u})(s) = 0 \right\}.
\end{aligned}$$

The "inactive set" is given by $\mathfrak{I} := \Gamma \setminus (\mathfrak{A}^+ \cup \mathfrak{A}^- \cup \mathfrak{B}^+ \cup \mathfrak{B}^-)$. One can show that $(\cdot)_+ : L^2(\Gamma) \to L^2(\Gamma)$ is directionally differentiable at any $w \in L^2(\Gamma)$ in any direction $h \in L^2(\Gamma)$. However, if $|\mathfrak{B}^+ \cup \mathfrak{B}^-| > 0$, then $(\cdot)'_+(w;\cdot) : L^2(\Gamma) \to L^2(\Gamma)$ is non-linear. This corresponds to a lack of "strict complementarity" in non-linear programming. Physically speaking, strict complementarity fails, i.e., $|\mathfrak{B}^+ \cup \mathfrak{B}^-| > 0$, when there is pinning ($\lambda = \pm P_{\text{pin}}$) and yet no normal force acts on the boundary ($C\mathbf{u} = 0$). This unstable situation may appear pathological, however, it cannot be ruled out (both from a mathematical as well as physical standpoint); see the magenta nodes in Figure 7. For this reason, the control problem cannot be handled directly with standard techniques of PDE-constrained optimization. In general, we note that pinning/biactivity is essential for problems in which one would like to exactly match a desired shape; see, for instance, the last numerical experiment.

In order to derive optimality conditions for (P), we work with (2.1) in solenoidal form, i.e., we restrict the set of test functions in the first equation in (2.1) to the space

$$\mathbb{V}_{\text{sol}} := \left\{ \mathbf{v} \in \mathbb{V} \,|\, B\mathbf{v} = 0 \right\}$$

and consider $A : \mathbb{V}_{\text{sol}} \to \mathbb{V}_{\text{sol}}^*$. The operators C, F, F_0 are also redefined accordingly. Note that this restriction does not affect the coercivity of A. In solenoidal form, the non-unique pressure variable p disappears and (2.1) can be modeled as a generalized equation. For this purpose and for convenience, we define $\varphi : \mathbb{V}_{\text{sol}} \to \mathbb{R}$ by

$$\varphi(\mathbf{u}) := P_{\text{pin}}\big(\|\cdot\|_{L^1(\Gamma)} \circ C\big)(\mathbf{u}), \quad \mathbf{u} \in \mathbb{V}_{\text{sol}}.$$

Then the solenoidal form of (2.1) is as follows:

$$A\mathbf{u} + \partial\varphi(\mathbf{u}) \ni F(E). \tag{2.2}$$

2.2 *An MPEC in function space*

We now return to the control problem (P), which may be rewritten using the solenoidal setting. As a consequence, both the pressure variable p and the pinning variable λ, due to (2.2), become implicit. Therefore, we henceforth consider objectives $\widehat{\mathfrak{J}}(E,\mathbf{u})$ only (rather than $\mathfrak{J}(E,z)$ as in (P)). Unless otherwise noted, we assume that the objective $\widehat{\mathfrak{J}} : \mathcal{E} \times \mathbb{V}_{\text{sol}} \to \mathbb{R}$ is continuously Fréchet differentiable and the set of admissible controls $\mathcal{E}_{ad}$ is nonempty, closed and convex. Finally, we will assume that $\widehat{\mathfrak{J}}$ satisfies the usual assumptions, cf. Theorem 3.1, needed to obtain the existence

of a minimizer to:

$$\begin{aligned} &\min\ \widehat{\mathfrak{J}}(E,\mathbf{u}) \text{ over } (E,\mathbf{u}) \in \mathfrak{E}\times\mathbb{V}_{\rm sol} \\ &\text{s.t.} \\ &\quad A\mathbf{u}+\partial\varphi(\mathbf{u}) \ni F(E),\ E\in\mathfrak{E}_{ad}. \end{aligned} \tag{2.3}$$

Since A is a coercive symmetric bounded linear operator, and therefore strongly monotone, and $\partial\varphi$ is a maximal monotone operator defined on all of $\mathbb{V}_{\rm sol}$, a real Hilbert space, the operator $A+\partial\varphi$ is surjective, see e.g., [6, Theorems 2, 2′] or [41, 42]. Moreover, one can either apply a classical result of Minty [39], see, e.g., [53, Theorem 26.A], or standard arguments from variational inequalities, see, e.g., the well-known monograph [37], to demonstrate that the solution operator $\widehat{\Phi} := (A+\partial\varphi)^{-1}$, with $\widehat{\Phi}:\mathbb{V}^*_{\rm sol}\to\mathbb{V}_{\rm sol}$, is Lipschitz continuous. Furthermore, as F is a continuous affine operator, the mapping $\Phi := \widehat{\Phi}\circ F$ is Lipschitz continuous from $\mathfrak{E}$ into $\mathbb{V}_{\rm sol}$. This allows us to rewrite the MPEC (2.3) in reduced form as

$$\min\ \mathfrak{J}(E) := \widehat{\mathfrak{J}}\big(E,\Phi(E)\big) \text{ over } E\in\mathfrak{E}_{ad}. \tag{2.4}$$

We are then left with a non-smooth non-convex optimization problem with convex control constraints.

3. Dual optimality conditions via limiting regularization

In order to derive dual optimality conditions, we use a regularization approach in which we smooth the $L^1(\Gamma)$-norm in φ. This leads to an approximation of the control problem (2.4) via a sequence of more tractable problems. After demonstrating existence and providing a general approximation framework, we derive first-order multiplier-based stationarity conditions for (2.4). We will use the notation $\overset{X}{\rightharpoonup}$ or simply $\rightharpoonup$, when X is clear in context, to denote weak convergence in some space X. As mentioned, our arguments rely heavily on the approach in the monograph by Barbu [4].

3.1 *An existence theorem*

In the following, we provide a basic existence theorem that includes both (2.4) as well as our approximating problems.

Theorem 3.1 *Let $M:\mathbb{V}_{\rm sol}\rightrightarrows\mathbb{V}^*_{\rm sol}$ be a maximal monotone operator and assume that $\widehat{\mathfrak{J}}:\mathfrak{E}\times\mathbb{V}_{\rm sol}\to\overline{\mathbb{R}}$ is bounded from below, weakly lower-semicontinuous in $\mathfrak{E}$/strongly lower-semicontinous in $\mathbb{V}_{\rm sol}$, and either $\mathfrak{E}_{ad}$ is bounded or $\widehat{\mathfrak{J}}$ is partially coercive with respect to $\mathfrak{E}_{\rm ad}$, i.e., for every sequence $(E_k,\mathbf{u}_k)\in\mathfrak{E}\times\mathbb{V}_{\rm sol}$ with $\|E_k\|_{\mathfrak{E}}\to\infty$ it holds that $\widehat{\mathfrak{J}}(E_k,\mathbf{u}_k)\to\infty$. Moreover, assume that the following problem has a feasible point:*

$$\inf\Big\{\widehat{\mathfrak{J}}(E,\mathbf{u}) \text{ over } (E,\mathbf{u})\in\mathfrak{E}\times\mathbb{V}_{\rm sol} : A\mathbf{u}+M(\mathbf{u})\ni F(E),\ E\in\mathfrak{E}_{ad}\Big\}. \tag{3.1}$$

Then there exists a minimizer $(E,\mathbf{u})\in\mathfrak{E}_{\rm ad}\times\mathbb{V}_{\rm sol}$ of (3.1).

Proof. Using the same arguments leading to the derivation of (2.4), it follows that the map $\Upsilon := (A+M)^{-1}$ is Lipschitz from $\mathbb{V}^*_{\rm sol}$ to $\mathbb{V}_{\rm sol}$. In addition, $F_0:\mathfrak{E}\to\mathbb{V}^*_{\rm sol}$ is compact. Therefore, the reduced objective $\mathfrak{J}(E) := \widehat{\mathfrak{J}}(E,\Upsilon(F(E))$ is weakly lower-semicontinuous in E. The rest of the proof is a standard application of the direct method of calculus of variations. □

REMARK 3.2 As the $L^1(\Gamma)$-norm is continuous and convex, the set-valued mapping $\partial(\|\cdot\|_{L^1(\Gamma)} \circ C)(\cdot) = C^*(\partial\|\cdot\|_{L^1(\Gamma)} \circ C)(\cdot)$ is maximal monotone, see, e.g., [41]. Therefore, (2.4) has a solution provided the chosen objective $\widehat{\mathfrak{J}}$ satisfies the (usual) conditions required in Theorem 3.1.

3.2 *Smoothing the $L^1(\Gamma)$-norm*

In the following, we let $\psi : \mathbb{R} \to \mathbb{R}$, be given by $\psi(r) := |r|$ and

$$\Psi(v) := \|v\|_{L^1(\Gamma)} = \int_\Gamma \psi(v(s))ds, \ \ v \in L^1(\Gamma).$$

Our regularization ansatz is essentially related to the conditions in [4, Chap. 2]. In fact, let $\Psi_\alpha : L^2(\Gamma) \to \overline{\mathbb{R}}$ for $\alpha > 0$ be a family of functionals that have the following properties:

(i) For all $\alpha > 0$, Ψ_α is a convex and continuously Frèchet differentiable functional on $L^2(\Gamma)$. Moreover, Ψ'_α is continuously Frèchet differentiable from $L^r(\Gamma)$ into $L^{r'}(\Gamma)$ with $r > 2$ and $1/r + 1/r' = 1$.

(ii) There exists a constant $\vartheta > 0$ such that for all $v \in L^2(\Gamma)$ and $\alpha > 0$: $\Psi_\alpha(v) \geqslant -\vartheta(\|v\|_{L^2(\Gamma)} + 1)$.

(iii) For all $\alpha_k \downarrow 0$ and for all $v \in L^2(\Gamma)$, it holds that $\Psi_{\alpha_k}(v) \to \Psi(v)$.

(iv) For all $\alpha_k \downarrow 0$, $v \in L^2(\Gamma)$, and $\{v_k\} \subset L^2(\Gamma)$ such that $v_k \rightharpoonup v$, it holds that $\liminf_{k\to+\infty} \Psi_{\alpha_k}(v_k) \geqslant \Psi(v)$.

(v) For every bounded set $\mathfrak{M} \subset \mathbb{V}^*_{\text{sol}}$, the set

$$\bigcup_{\mathbf{y}\in\mathfrak{M}} \left\{(\mathbf{u}, \alpha) \in \mathbb{V}_{\text{sol}} \times (0, 1] \,\middle|\, A\mathbf{u} + C^*\Psi'_\alpha(C\mathbf{u}) = \mathbf{y}\right\}$$

is bounded in $\mathbb{V}_{\text{sol}} \times \mathbb{R}$.

Here, condition (i) is essential for the derivation of an adjoint equation in the first-order optimality conditions of the smoothed version of (2.4), whereas (ii) along with convexity and continuity ensure that Ψ'_α is a maximal monotone operator. Conditions (iii) and (iv) are a slight weakening of the usual requirements for Γ-convergence, i.e., epi-convergence. Finally, (v) ensures the uniform boundedness of the states $\mathbf{u}_\alpha$ in the approximating problems with respect to $\alpha > 0$. For a general class of integral functionals that satisfies these conditions, we refer the reader to the Appendix. A concrete example of such a Ψ_α is given in Section 4.3. For the coming discussion, it suffices to assume that following structure:

1. $\psi_\alpha : \mathbb{R} \to \mathbb{R}$ is a convex, twice continuously differentiable approximation of the absolute value ($\psi(r) := |r|$). It has the form

$$\psi_\alpha(r) := \alpha\widetilde{\psi}(\alpha^{-1}r) + \varepsilon_\alpha,$$

where $\widetilde{\psi} : \mathbb{R} \to \mathbb{R}$ is convex, twice continuously differentiable with $\widetilde{\psi}(r) \geqslant \psi(r) = |r|$, $\widetilde{\psi}''(r) < c$ ($c \in \mathbb{R}$) and satisfies certain growth properties (see Proposition 5.1); ε_α is a null sequence and $\alpha > 0$.

2. $\Psi_\alpha(v)$ is a smooth integral functional that approximates the L^1 norm. It has the form

$$\Psi_\alpha(v) := \int_\Gamma \psi_\alpha\big(v(s)\big)ds, \quad v \in L^2(\Gamma).$$

3.3 *A class of approximating optimization problems*

Using the smoothing of the $L^1(\Gamma)$-norm from the previous subsection, we define the following class of approximations to (2.4):

$$\min \left\{ \widehat{\mathfrak{J}}(E, \mathbf{u}) \text{ over } (E, \mathbf{u}) \in \mathfrak{E} \times \mathbb{V}_{\text{sol}} : A\mathbf{u} + P_{\text{pin}} C^* \Psi'_\alpha(C\mathbf{u}) = F(E),\ E \in \mathfrak{E}_{ad} \right\}. \tag{3.2}$$

The nonlinear equation:

$$A\mathbf{u} + P_{\text{pin}} C^* \Psi'_\alpha(C\mathbf{u}) = F(E), \tag{3.3}$$

will be referred to as the smoothed EWOD problem. The difference between (2.1) and (3.3) can be best understood by formally returning to the strong formulation (1.1). By letting $\lambda = \widetilde{\psi}'(\alpha^{-1}\mathbf{u} \cdot \boldsymbol{\nu})$ and replacing (1.1c)-(1.1d) by

$$p\boldsymbol{\nu} - E\boldsymbol{\nu} - \kappa\boldsymbol{\nu} - P_{\text{pin}} \widetilde{\psi}'(\alpha^{-1}\mathbf{u} \cdot \boldsymbol{\nu})\boldsymbol{\nu} - D_{\text{visc}}[\mathbf{u} \cdot \boldsymbol{\nu}]\boldsymbol{\nu} = 0,$$

the associated weak and then solenoidal form yields (3.3). Typically, see Section 4.3, one would choose a smoothing in which $\widetilde{\psi}'(r) = 1$ for $r \geqslant 1$ and $\widetilde{\psi}'(r) = -1$ for $r \leqslant -1$. As a consequence, after scaling, we introduce a type of friction that "slows" the motion of the droplet. Indeed, for the non-smooth model, $1 >> |\mathbf{u} \cdot \boldsymbol{\nu}| > 0$ would imply $\lambda = \pm 1$, whereas here $|\lambda| < 1$ (see Figure 2 below).

In the following result, we demonstrate the existence of a solution to (3.2) and the consistency of the approximation with the original problem (2.3) when $\alpha \downarrow 0$.

Proposition 3.3 (Consistency of the Approximation) *Let $\widehat{\mathfrak{J}}$ be as in Theorem 3.1 and $\alpha > 0$. Then (3.2) admits a minimizer $(E_\alpha, \mathbf{u}_\alpha)$ and for any sequence $\{\alpha_k\}_{k=1}^\infty$ with $\alpha_k \downarrow 0$, there exists a subsequence $\{\alpha_{k_l}\}_{l=1}^\infty$ and a point $(E^*, \mathbf{u}^*)$ such that $E_{\alpha_{k_l}} \overset{\mathfrak{E}}{\rightharpoonup} E^*$ and $\mathbf{u}_{\alpha_{k_l}} \overset{\mathbb{V}_{\text{sol}}}{\to} \mathbf{u}^*$ as $l \to \infty$, where (E^*, u^*) is a minimizer of (2.3).*

Proof. Since $(\Psi_\alpha \circ C) : \mathbb{V}_{\text{sol}} \to \mathbb{R}$ is convex, differentiable, and continuous, its gradient is maximal monotone. Therefore, there exists a unique solution $\mathbf{u}_\alpha$ to (3.3) for all $E \in \mathfrak{E}_{ad}$ and $\alpha > 0$, cf. proof of Theorem 3.1. Hence, (3.2) always has a feasible point. The existence of a solution $(E_\alpha, \mathbf{u}_\alpha)$ to (3.2) for any $\alpha > 0$ then follows from Theorem 3.1. Using the ellipticity of A, compactness of $F : E \to \mathbb{V}^*_{\text{sol}}$, and variational convergence in ((iii)–(iv)) for $\Psi_{\alpha_k} \to \Psi$ one can show that $\mathbf{u}_{\alpha_k} \overset{\mathbb{V}_{\text{sol}}}{\to} \mathbf{u}$ (strongly) along any sequence $\alpha_k \downarrow 0$. Alternatively, one can verify the conditions of [4, Theorem 2.2, p. 41].

Continuing, since $\mathfrak{J}$ is assumed to be partially coercive (or $\mathfrak{E}_{\text{ad}}$ is bounded), it follows that the set of controls $\{E_\alpha\}_{\alpha>0}$ is bounded in $\mathfrak{E}$. Thus, $\{u_\alpha\}_{\alpha>0}$ is bounded in $\mathbb{V}_{\text{sol}}$. Therefore, for any sequence $\{\alpha_k\}_{k=1}^\infty$ with $\alpha_k \downarrow 0$, there exists a subsequence $\{\alpha_{k_l}\}_{l=1}^\infty$ and a point $(E^*, \mathbf{u}^*)$ such that $E_{\alpha_{k_l}} \overset{\mathfrak{E}}{\rightharpoonup} E^*$ and $\mathbf{u}_{\alpha_{k_l}} \overset{\mathbb{V}_{\text{sol}}}{\to} \mathbf{u}^*$ as $l \to \infty$. It remains to show that $(E^*, \mathbf{u}^*)$ is also a solution.

Since $\mathfrak{E}_{ad}$ is closed and convex, it is weakly closed. Therefore, $E^* \in \mathfrak{E}_{ad}$. Moreover, it follows from [4, Theorem 2.2, p.41] that $\mathbf{u}^*$ satisfies $A\mathbf{u}^* + P_{\text{pin}} C^* (\partial \|\cdot\|_{L^1(\Gamma)} \circ C)(\mathbf{u}) \ni F(E^*)$. Hence, $(E^*, \mathbf{u}^*)$ is feasible for (2.3).

Finally, taking $(E', \mathbf{u}')$ to be any minimizer of (2.3), we can use the same limiting argument above to show that if $A\mathbf{u}'_\alpha + P_{\text{pin}}C^*\Psi'_\alpha(C\mathbf{u}'_\alpha) \ni F(E')$, then we can select a subsequence of $\{\alpha_{k_{l_n}}\}_{n=1}^{\infty}$ such that $\mathbf{u}'_{\alpha_{k_{l_n}}} \to \mathbf{u}'$ as $n \to +\infty$. It follows that

$$\mathcal{J}(E', \mathbf{u}') \leqslant \mathcal{J}(E^*, \mathbf{u}^*) \leqslant \liminf_{n\to+\infty} \mathcal{J}(E_{\alpha_{k_{l_n}}}, \mathbf{u}_{\alpha_{k_{l_n}}}) \leqslant \liminf_{n\to+\infty} \mathcal{J}(E', \mathbf{u}'_{\alpha_{k_{l_n}}}) = \mathcal{J}(E', \mathbf{u}');$$

as was to be shown. □

Despite being a consistent approximation, Ψ_α does not guarantee that we can reach every solution pair $(E', \mathbf{u}')$ to (2.3) with sequences of approximating solutions. Moreover, since the approximating problems (3.2) themselves are not convex, the consistency result is primarily of theoretical interest. Indeed, we have no guaranteed way of numerically calculating globally optimal pairs $(E_\alpha, \mathbf{u}_\alpha)$. Even ensuring local optimality by numerical means is typically out of reach or at least very expensive. Nevertheless, under the assumption that $\mathcal{E}_{\text{ad}}$ is bounded, we can extend the consistency result to include the convergence of approximating *stationary points*; which is then the basis for our numerical method.

We finish this subsection with a sensitivity result for the solution mapping of the smoothed EWOD system (3.3).

Proposition 3.4 *Let $\Phi_\alpha : \mathcal{E} \to \mathbb{V}_{\text{sol}}$ with $E \mapsto \Phi_\alpha(E)$ be defined by*

$$\Phi_\alpha(E) := (A\mathbf{u} + P_{\text{pin}}C^*\Psi'_\alpha \circ C)^{-1}F(E).$$

Then Φ_α is Fréchet differentiable. The Fréchet derivative of Φ_α at E in direction $\delta E \in \mathcal{E}$ is given by $\delta\mathbf{u} = \Phi'_\alpha(C\mathbf{u})\delta E$, the unique solution of the sensitivity equation

$$\big(A + P_{\text{pin}}C^*\Psi''_\alpha(C\mathbf{u})C\big)\mathbf{v} = F_0(\delta E).$$

Proof. The linearization of (3.3) is given by $(A + P_{\text{pin}}C^*\Psi''_\alpha(C\mathbf{u})C)\delta\mathbf{u} - F_0(\delta E) = 0$. To see that $(A + P_{\text{pin}}C^*\Psi''_\alpha(C\mathbf{u})C)$ is a linear isomorphism, we apply the same arguments used to derive the reduced control problems (3.4) and (2.4). Indeed, A is a bounded linear strongly monotone operator and $C^*\Psi''_\alpha(C\mathbf{u})C$ is linear and monotone; since Ψ_α is convex, continuous and twice Fréchet differentiable. Therefore, $(A + P_{\text{pin}}C^*\Psi''_\alpha(C\mathbf{u})C)^{-1} : \mathbb{V}^*_{\text{sol}} \to \mathbb{V}_{\text{sol}}$ is a bijection. The rest follows from the implicit function theorem, cf. [54]. □

3.4 *First-order conditions*

In this subsection, we derive dual first-order optimality conditions for (2.4). In light of Proposition 3.4, we can somewhat simplify the analysis by first deriving a smoothed version of (2.4). Indeed, notice that $C^*\Psi'_\alpha(C\mathbf{u}) = \partial(\Psi_\alpha \circ C)(\mathbf{u})$ is a maximal monotone operator. For some $E \in \mathcal{E}$ let $\mathbf{u}_\alpha(E) = \Phi_\alpha(E) := (A + P_{\text{pin}}\partial(\Psi_\alpha \circ C))^{-1}(F(E))$. Due to the strong monotonicity of $A : \mathbb{V}_{\text{sol}} \to \mathbb{V}^*_{\text{sol}}$ and compactness of $F : \mathcal{E} \to \mathbb{V}^*_{\text{sol}}$, the solenoidal velocity field $\mathbf{u}_\alpha$ depends completely Lipschitz continuously on the control E (from $\mathcal{E}$ to $\mathbb{V}_{\text{sol}}$). That is, if $E_n \rightharpoonup E$ in $\mathcal{E}$ then $\mathbf{u}_\alpha(E_n) \to \mathbf{u}_\alpha(E)$ in $\mathbb{V}_{\text{sol}}$ and $\mathbf{u}_\alpha(\cdot) : \mathcal{E} \to \mathbb{V}_{\text{sol}}$ is Lipschitz continuous. Hence, we obtain the smoothed version of (2.4):

$$\min \mathcal{J}_\alpha(E) := \widehat{\mathcal{J}}\big(E, \Phi_\alpha(E)\big) \text{ over } E \in \mathcal{E}_{ad}. \tag{3.4}$$

We continue this section by deriving first-order multiplier-based optimality conditions for both the approximating control problems (3.4) and, subsequently, upon passing to the limit as $\alpha \downarrow 0$, for (2.4). We henceforth assume that

- $\widehat{\mathfrak{J}}$ is continuously Fréchet differentiable,
- $\partial\widehat{\mathfrak{J}} : \mathcal{E} \times \mathbb{V}_{\text{sol}} \to \mathcal{E}^* \times \mathbb{V}_{\text{sol}}^*$, where $\partial\widehat{\mathfrak{J}} = (\partial_E \widehat{\mathfrak{J}}, \partial_{\mathbf{u}} \widehat{\mathfrak{J}})$, is bounded,
- $\mathcal{E}_{ad}$ is bounded.

Given an optimal solution $(E_\alpha, \mathbf{u}_\alpha)$ to (3.4), we can use Proposition 3.4 to derive the following (standard) first-order optimality condition for (3.4) and therefore, for (3.2):

$$\left\langle \partial_E \mathfrak{J}(E_\alpha, \mathbf{u}_\alpha) + F_0^* \Phi_\alpha'(E_\alpha)^* \partial_{\mathbf{u}} \mathfrak{J}(E_\alpha, \mathbf{u}_\alpha), E - E_\alpha \right\rangle \geqslant 0, \quad \forall E \in \mathcal{E}_{ad}. \tag{3.5}$$

By letting $\mathbf{w}_\alpha = \Phi_\alpha'(E_\alpha)^*(-\partial_{\mathbf{u}} \widehat{\mathfrak{J}}(E_\alpha, \mathbf{u}_\alpha))$, the next proposition follows immediately from (3.5), which is equivalent to $\mathbf{w}_\alpha$ solving (3.7).

Proposition 3.5 *Suppose $(E_\alpha, \mathbf{u}_\alpha) \in \mathcal{E} \times \mathbb{V}_{\text{sol}}$ is a (locally) optimal solution of (3.2). Then the following dual optimality condition holds:*

$$\left\langle \partial_E \mathfrak{J}(E_\alpha, \mathbf{u}_\alpha) - F_0^* \mathbf{w}_\alpha, E - E_\alpha \right\rangle \geqslant 0, \quad \forall E \in \mathcal{E}_{ad} \tag{3.6}$$

where $\mathbf{w}_\alpha \in \mathbb{V}_{\text{sol}}$ solves the adjoint equation

$$A^* \mathbf{w}_\alpha + C^* \Psi_\alpha''(C\mathbf{u}_\alpha) C \mathbf{w}_\alpha = -\partial_{\mathbf{u}} \mathfrak{J}(E_\alpha, \mathbf{u}_\alpha). \tag{3.7}$$

From now on we call $\mathbf{w}_\alpha$ the adjoint state associated with (3.7). Proposition 3.5 leads us to the following definition.

DEFINITION 3.6 (Stationary Points) Given some $\alpha > 0$, we say that the triple $(E_\alpha, \mathbf{u}_\alpha, \mathbf{w}_\alpha)$ is a stationary point of (3.2) provided $(E_\alpha, \mathbf{u}_\alpha)$ is feasible and $(E_\alpha, \mathbf{u}_\alpha, \mathbf{w}_\alpha)$ satisfies (3.3), (3.6)–(3.7).

Based on Definition 3.6, we derive a limiting stationarity system first for the original problem (2.3), or equivalently, (2.4). As stationary points according to Definition 3.6 can be computed numerically upon discretization, this limiting procedure also serves the purpose of a convergence proof for the associated numerical algorithm. As a corollary, since every optimal solution to (3.2) is stationary, we acquire by virtue of Proposition 3.3, a first-order optimality system for those solutions to (2.4) which can be reached by weak accumulation points of approximations $\{(E_\alpha, \mathbf{u}_\alpha)\}$.

Lemma 3.7 (Boundedness of Stationary Points) *Let $\{(E_\alpha, \mathbf{u}_\alpha, \mathbf{w}_\alpha)\}_{\alpha>0} \subset \mathcal{E}_{ad} \times \mathbb{V}_{\text{sol}} \times \mathbb{V}_{\text{sol}}$ be the set of all stationary points for the approximating problems (3.2). Then $\{(E_\alpha, \mathbf{u}_\alpha, \mathbf{w}_\alpha)\}_{\alpha>0}$ is bounded in $\mathcal{E}_{ad} \times \mathbb{V}_{\text{sol}} \times \mathbb{V}_{\text{sol}}$.*

Proof. Since $\mathcal{E}_{\text{ad}}$ is bounded, $\{E_\alpha\}_{\alpha>0}$ is bounded in $\mathcal{E}$. Continuing, it follows from property (v), cf. Equation (5.3), that $\{\mathbf{u}_\alpha\}_{\alpha>0}$ is bounded in $\mathbb{V}_{\text{sol}}$. Similarly, since $\partial_{\mathbf{u}} \mathfrak{J}$ maps bounded sets into bounded sets and A is symmetric, we obtain the boundedness of $\{\mathbf{w}_\alpha\}_{\alpha>0}$ in $\mathbb{V}_{\text{sol}}$. □

Theorem 3.8 (Convergence of Stationary Points) *Let $\alpha_k \downarrow 0$ and define $(E_k, \mathbf{u}_k, \mathbf{w}_k) := (E_{\alpha_k}, \mathbf{u}_{\alpha_k}, \mathbf{w}_{\alpha_k})$ to be a sequence of associated stationary points. Then there exists a subsequence $\{(E_{k_l}, \mathbf{u}_{k_l}, \mathbf{w}_{k_l})\}_{l=1}^{\infty}$ and a triple $(E^*, \mathbf{u}^*, \mathbf{w}^*)$ such that*

$$E_{k_l} \overset{\mathcal{E}}{\rightharpoonup} E^*, \quad \mathbf{u}_{k_l} \overset{\mathbb{V}_{\text{sol}}}{\to} \mathbf{u}^*, \quad \mathbf{w}_{k_l} \overset{\mathbb{V}_{\text{sol}}}{\rightharpoonup} \mathbf{w}^*, \text{ as } l \to +\infty,$$

where $(E^*, \mathbf{u}^*)$ *is feasible for* (2.3). *Moreover, there exist* $m^*, \mathfrak{J}_{\mathbf{u}}^* \in \mathbb{V}_{\mathrm{sol}}^*$ *such that*

$$\partial_{\mathbf{u}} \mathfrak{J}(E_{k_l}, \mathbf{u}_{k_l}) \overset{\mathbb{V}_{\mathrm{sol}}^*}{\rightharpoonup} \mathfrak{J}_{\mathbf{u}}^* \text{ and } m_{k_l} := C^* \Psi''_{\alpha_{k_l}}(\mathbf{u}_{k_l}) C \mathbf{w}_{k_l} \overset{\mathbb{V}_{\mathrm{sol}}^*}{\rightharpoonup} m^*.$$

In addition, it holds that

$$A^* \mathbf{w}^* + P_{\mathrm{pin}} m^* = -\mathfrak{J}_{\mathbf{u}}^*, \tag{3.8}$$

$$\liminf_{l \to +\infty} \langle m_{k_l}, \mathbf{w}_{k_l} \rangle \geqslant 0, \tag{3.9}$$

$$\liminf_{l \to +\infty} \left\langle \partial_E \mathfrak{J}(E_{k_l}, \mathbf{u}_{k_l}) - F_0^* \mathbf{w}_{k_l}, E - E_{k_l} \right\rangle \geqslant 0, \quad \forall E \in \mathcal{E}_{ad}. \tag{3.10}$$

Proof. It follows from Lemma 3.7 that we can select a subsequence $\{(E_{\alpha_{k_l}}, \mathbf{u}_{\alpha_{k_l}}, \mathbf{w}_{\alpha_{k_l}})\}_{l=1}^{\infty} \in \mathcal{E} \times \mathbb{V}_{\mathrm{sol}} \times \mathbb{V}_{\mathrm{sol}}$ and a triple $(E^*, \mathbf{u}^*, \mathbf{w}^*)$ such that $(E_{\alpha_{k_l}}, \mathbf{u}_{\alpha_{k_l}}, \mathbf{w}_{\alpha_{k_l}}) \rightharpoonup (E^*, \mathbf{u}^*, \mathbf{w}^*)$ in $\mathcal{E} \times \mathbb{V}_{\mathrm{sol}} \times \mathbb{V}_{\mathrm{sol}}$.

Since $\mathcal{E}_{ad}$ is closed and convex, and therefore weakly closed, $E^* \in \mathcal{E}_{ad}$. Recalling the argument in Proposition 3.3, i.e., [4, Theorem 2.2, p. 41], it follows that $\mathbf{u}^*$ solves (2.2) with $E = E^*$. In fact, it holds that $\mathbf{u}_{k_l} \to \mathbf{u}^*$ strongly in $\mathbb{V}_{\mathrm{sol}}$.

Next, since $\mathbf{w}_{k_l} \rightharpoonup \mathbf{w}^*$ in $\mathbb{V}_{\mathrm{sol}}^*$ and $\{\partial_{\mathbf{u}} \mathfrak{J}(E_{k_l}, \mathbf{u}_{k_l})\}_{l=1}^{\infty}$ is bounded in $\mathbb{V}_{\mathrm{sol}}^*$, we obtain the boundedness of $\{m_{k_l}\}_{l=1}^{\infty}$ with

$$m_{k_l} := C^* \Psi''_{\alpha_{k_l}}(C \mathbf{u}_{k_l}) C \mathbf{w}_{k_l}.$$

Then passing to the weak limit along a subsequence if necessary, it holds that $A^* \mathbf{w}^* + m^* = -\mathfrak{J}_{\mathbf{u}}^*$, this yields (3.8). The inequality condition (3.9), follows immediately by definition of m_k and $\mathbf{w}_k$:

$$\langle m_{k_l}, \mathbf{w}_{k_l} \rangle = \int_{\Gamma} \alpha_{k_l}^{-1} \widetilde{\psi}''\big(\alpha_{k_l}^{-1}(C \mathbf{u}_{k_l})(s)\big) \big|(C \mathbf{w}_{k_l})(s)\big|^2 ds \geqslant 0.$$

Finally, taking the limit inferior of (3.6) yields: (3.10). □

Without additional compactness assumptions on the gradient of the objective functional $\widehat{\mathfrak{J}}$ or if the control space $\mathcal{E}$ is not finite dimensional, it is difficult to refine (3.8)–(3.10) in the general setting. A special case, which covers our example objective functionals, is considered in the following result.

Corollary 3.9 *Let* H *be a Hilbert space, let* $L : \mathbb{V}_{\mathrm{sol}} \to H$ *be a compact bounded linear operator, and let* $\widehat{\mathfrak{J}} : \mathcal{E} \times \mathbb{V}_{\mathrm{sol}} \to \mathbb{R}$ *be given by*

$$\widehat{\mathfrak{J}}(E, \mathbf{u}) := \frac{1}{2} \|L \mathbf{u} - u_b\|_H^2 + \frac{\nu}{2} \|E\|_{\mathcal{E}}^2,$$

where $\nu > 0$ *and* $u_b \in H$. *Then we obtain the following limiting stationarity conditions:*
Let $\alpha_k \downarrow 0$ *and define* $(E_k, \mathbf{u}_k, \mathbf{w}_k) := (E_{\alpha_k}, \mathbf{u}_{\alpha_k}, \mathbf{w}_{\alpha_k})$ *to be a sequence of associated stationary points. Then there exists a subsequence* $\{(E_{k_l}, \mathbf{u}_{k_l}, \mathbf{w}_{k_l})\}_{l=1}^{\infty}$ *and a triple* $(E^*, \mathbf{u}^*, \mathbf{w}^*)$ *such that* $E_{k_l} \overset{\mathcal{E}}{\rightharpoonup} E^*, \mathbf{u}_{k_l} \overset{\mathbb{V}_{\mathrm{sol}}}{\to} \mathbf{u}^*, \mathbf{w}_{k_l} \overset{\mathbb{V}_{\mathrm{sol}}}{\rightharpoonup} \mathbf{w}^*$, *as* $l \to +\infty$, *where* $(E^*, \mathbf{u}^*)$ *is feasible for* (2.3). *Moreover, there exists an* $m^* \in \mathbb{V}_{\mathrm{sol}}^*$ *such that* $m_{k_l} := C^* \Psi''_{\alpha_{k_l}}(\mathbf{u}_{k_l}) C \mathbf{w}_{k_l} \overset{\mathbb{V}_{\mathrm{sol}}^*}{\rightharpoonup} m^*$. *In addition, we have:*

$$A^* \mathbf{w}^* + P_{\mathrm{pin}} m^* = L^*(u_b - L \mathbf{u}^*), \tag{3.11a}$$

$$\langle m^*, \mathbf{w}^* \rangle \geqslant 0, \tag{3.11b}$$

$$\langle \nu E^* - F_0^* \mathbf{w}^*, E - E^* \rangle \geqslant 0, \ \forall E \in \mathcal{E}_{ad}. \tag{3.11c}$$

Proof. The proof follows immediately from the proof of Theorem 3.8. Indeed, we have $\partial_{\mathbf{u}}\mathfrak{J}(E_{k_l}, \mathbf{u}_{k_l}) = L^*(L\mathbf{u}_{k_l} - u_b)$ and $\partial_E \mathfrak{J}(E_{k_l}, \mathbf{u}_{k_l}) = \nu E_{k_l}$. Therefore, due to the compactness of L, $L^*(L\mathbf{u}_{k_l} - u_b) \to L^*(L\mathbf{u}^* - u_b)$ strongly in $\mathbb{V}^*_{\text{sol}}$. This yields (3.11a). Moreover, we have for each $E \in \mathfrak{E}_{ad}$ that

$$0 \leqslant \left\langle \partial_E \mathfrak{J}(E_{k_l}, u_{k_l}) - F_0^* \mathbf{w}_{k_l}, E - E_{k_l} \right\rangle = \langle -F_0^* \mathbf{w}_{k_l}, E - E_{k_l} \rangle + \nu \langle E_{k_l}, E - E_{k_l} \rangle.$$

Since $F_0^* : \mathbb{V}_{\text{sol}} \to \mathfrak{E}$ is compact, $\langle -F_0^* \mathbf{w}_{k_l}, E - E_{k_l} \rangle \to \langle -F_0^* \mathbf{w}^*, E - E^* \rangle$. Moreover, due to the weak-lower semicontinuity of the $\mathfrak{E}$-norm, we have

$$0 \leqslant \liminf_{l \to \infty} \nu \langle E_{k_l}, E - E_{k_l} \rangle \leqslant \nu \langle E^*, E - E^* \rangle.$$

Combining these observations yields (3.11c).

In order to derive (3.11b), we test (3.7) with $\mathbf{w}_\alpha$. Given $m_\alpha := C^* \Psi''_\alpha(C\mathbf{u}_\alpha) C\mathbf{w}_\alpha$, where Ψ_α is a twice-continuously differentiable convex functional, we have $0 \leqslant \langle m_\alpha, \mathbf{w}_\alpha \rangle$. Moreover, it also follows from (3.7) and the explicit form of the objective that

$$0 \leqslant P_{\text{pin}} \langle m_\alpha, \mathbf{w}_\alpha \rangle = -\langle A^* \mathbf{w}_\alpha, \mathbf{w}_\alpha \rangle + \langle L^*(\mathbf{u}_b - L\mathbf{u}_\alpha), \mathbf{w}_\alpha \rangle.$$

Since A^* is symmetric, $\langle A^* \cdot, \cdot \rangle$ defines a continuous convex function on $\mathbb{V}_{\text{sol}}$. Then, in light of the compactness of L and L^*, we may pass to the limit superior (along an appropriately chosen subsequence) to obtain

$$0 \leqslant -\langle A^* \mathbf{w}^*, \mathbf{w}^* \rangle + \langle L^*(\mathbf{u}_b - L\mathbf{u}^*), \mathbf{w}^* \rangle = P_{\text{pin}} \langle m^*, \mathbf{w}^* \rangle,$$

as was to be shown. □

In addition to the more explicit stationarity conditions in Corollary 3.9, we can provide further refinements for the limiting multiplier m^* and limiting adjoint state $\mathbf{w}^*$. Note that these do not require special conditions on the objective functionals (such as in Corollary 3.9). Below, given a subset $S \subset \mathbb{R}^{n-1}$, $|S|$ denotes the $(n-1)$-dimensional Lebesgue measure of S.

Proposition 3.10 *In the context of Theorem 3.8, let $\mathfrak{A}_*^+$ and $\mathfrak{A}_*^-$ denote the strongly active sets associated with the limiting stationary point, and let*

$$\mathfrak{A}_* := \mathfrak{A}_*^+ \cup \mathfrak{A}_*^-.$$

Then, for all $\varepsilon > 0$, there exists a Lebesgue measurable set $\mathfrak{A}_*^\varepsilon \subset \mathfrak{A}_*$ with $|\mathfrak{A}_*^\varepsilon| \leqslant \varepsilon$ such that

$$0 = \langle m^*, \mathbf{v} \rangle, \quad \forall \mathbf{v} \in \mathbb{V}_{\text{sol}} : C\mathbf{v} = 0, \text{ a.e. on } \left\{ s \in \Gamma \mid (C\mathbf{u}^*)(s) = 0 \right\} \cup \mathfrak{A}_*^\varepsilon, \tag{3.12}$$

provided supp $\widetilde{\psi}'' \subset [-c, c]$ *for some $c > 0$.*

REMARK 3.11 (Limiting ε-almost C-stationarity) This condition is the infinite-dimensional analog of the finite-dimensional condition where the multiplier $m^* = 0$ on the inactive set. Together with (3.8)–(3.10) and the result in Proposition 3.12, the entire system constitutes a weak form of limiting ε-almost C-stationarity, see [31, 32]. In the case when there exists some function μ^* such that $m^* = C^* \mu^*$, then it would result in limiting ε-almost C-stationarity.

Proof. Without loss of generality, we denote the convergent subsequence of $\{m_k\}$ by the index k (according to the proof of Theorem 3.8). By the assumptions on $\widetilde{\psi}$, $\operatorname{supp}\psi''_{\alpha_k} \subset [-\alpha_k c, \alpha_k c]$ for some constant $c > 0$. Moreover, since $C : \mathbb{V}_{\mathrm{sol}} \to L^2(\Gamma)$ is compact, we may assume (taking a subsequence if necessary) that $C\mathbf{u}_k \to C\mathbf{u}^*$ pointwise almost everywhere on Γ. Therefore, for almost every $s \in \Gamma$ such that $C\mathbf{u}^*(s) \neq 0$, there exists a $K_s \in \mathbb{N}$ such that

$$\big|(C\mathbf{u}_k)(s) - (C\mathbf{u}^*)(s)\big| < \frac{1}{2}\big|(C\mathbf{u}^*)(s)\big| \text{ and } \psi''_{\alpha_k}(r) = 0, \quad \text{if } |r| \geqslant \frac{1}{2}\big|(C\mathbf{u}^*)(s)\big|,$$

for all $k \geqslant K_s$ and hence, α_k sufficiently small. In particular, we have here that $|(C\mathbf{u}_k)(s)| > |(C\mathbf{u}^*)(s)|/2$.

Hence, $\mu_k(s) := \psi''_{\alpha_k}((C\mathbf{u}_k)(s))(C\mathbf{w}_k)(s)$ vanishes almost everywhere for sufficiently large k, i.e., sufficiently small $\alpha_k > 0$, on $\mathfrak{A}_* := \{s \in \Gamma \,|\, (C\mathbf{u}^*)(s) \neq 0\}$. It follows from Egorov's theorem that for every $\varepsilon > 0$ there exists a subset $\mathfrak{A}_*^\varepsilon \subset \mathfrak{A}_*$ with $|\mathfrak{A}_*^\varepsilon| \leqslant \varepsilon$ such that μ_k converges uniformly on $\mathfrak{A}_* \setminus \mathfrak{A}_*^\varepsilon$. Then for any $\mathbf{v} \in \mathbb{V}_{\mathrm{sol}}$ with $C\mathbf{v} = 0$ almost everywhere on $\{s \in \Gamma \,|\, (C\mathbf{u}^*)(s) = 0\} \cup \mathfrak{A}_*^\varepsilon$ we have

$$0 = \lim_{k\to+\infty} \int_\Gamma \mu_k C\mathbf{v} ds = \lim_{k\to+\infty} \langle C^*\mu_k, \mathbf{v}\rangle = \lim_{k\to+\infty} \langle m_k, \mathbf{v}\rangle = \langle m^*, \mathbf{v}\rangle.$$

This concludes the proof. □

Since we currently do not have convergence of the inactive sets for the approximating problems in the sense of characteristic functions, we can only approximate the condition $C\mathbf{w}^* = 0$ a.e. on $\mathfrak{l}_* = \Omega \setminus \mathfrak{A}_*$, which is expected from similar stationarity conditions in the control of variational inequalities, see e.g. [23]. This is the subject of the next result.

Proposition 3.12 *Let $\alpha_k \downarrow 0$ and suppose that $\{(E_k, \mathbf{u}_k, \mathbf{w}_k)\}_{k=1}^\infty$ with $(E_k, \mathbf{u}_k, \mathbf{w}_k) := (E_{\alpha_k}, \mathbf{u}_{\alpha_k}, \mathbf{w}_{\alpha_k})$ is an associated sequence of stationary points that weakly converges in $\mathfrak{E} \times \mathbb{V}_{\mathrm{sol}} \times \mathbb{V}_{\mathrm{sol}}$ to $(E^*, \mathbf{u}^*, \mathbf{w}^*)$. Then the following holds:*

$$\lim_{k\to+\infty} \int_{\{s\in\Gamma\,|\,(C\mathbf{u}_k)(s)=0\}} \big|(C\mathbf{w}_k)(s)\big|^2 ds = 0.$$

Proof. Testing the adjoint equation (3.7) with $\mathbf{w}_\alpha$ and using the fact that A is coercive, the assumptions on Ψ_α and boundedness of the involved sequences yield the existence of some constant $\vartheta' > 0$ such that

$$0 \leqslant \int_\Gamma \widetilde{\psi}''\big(\alpha_k^{-1}(C\mathbf{u}_k)(s)\big)\big|(C\mathbf{w}_k)(s)\big|^2 ds \leqslant \alpha_k \vartheta',$$

where we recall that $\psi_\alpha(\alpha^{-1}r) := \alpha\widetilde{\psi}(\alpha^{-1}r) + \varepsilon_\alpha$, in which case $\psi''_\alpha(\alpha^{-1}r) = \alpha^{-1}\widetilde{\psi}''(\alpha^{-1}r)$. The assertion follows by passing to the limiting in k. □

4. Numerical experiments

We now propose an algorithm for the numerical realization of a strategy for (suboptimally) solving (2.4). In each time step, given the current state of the system, i.e., previous voltage pattern, free-boundary, velocity field, and pressure, we seek a feasible vector $(E, \mathbf{u}, p, \lambda)$ that reduces or even minimizes a given objective functional. As in the theoretical analysis of the control problem, the multivalued subdifferential mapping becomes an issue when developing numerical solution schemes. For this reason, we employ the same smoothing approach as above.

4.1 *Choosing an objective*

Until now, the objective function has been rather general. However, in order to realize a useful control, we consider the following four choices:

1. *Barycenter matching:*

$$\mathcal{J}^{i+1}(\mathbf{u}, E) = \frac{1}{2}\left\| \frac{1}{|\Omega^i|}\int_{\Omega^i} \big(x + \delta t_{i+1}\mathbf{u}(x)\big)\, dx - \mathbf{b}_d \right\|^2_{\mathbb{R}^2} + \frac{\zeta}{2}\|E\|^2_{\mathcal{E}}.$$

   Here, Ω^i is the support of the droplet in $\mathbb{R}^2$ at time step t_{i+1}. The integral expression is applied componentwise, which yields a vector in $\mathbb{R}^2$. The quantity $\mathbf{b}_d$ represents the coordinates of the desired barycenter. This term does not change at each time step. Finally, the last term is the cost of the control E with parameter $\zeta > 0$. In all the experiments we set the Tikhonov parameter $\zeta := 1e\text{-}8$, except in the final example where we set $\zeta := 1e\text{-}10$.
2. *Barycenter tracking:*
   The only difference to the previous functional is that $\mathbf{b}_d$ is replaced by a $\mathbf{b}_d^{i+1}$, where $(\mathbf{b}_d^1, \ldots, \mathbf{b}_d^T)$ represents a trajectory of desired barycenters.
3. *Matching the shape of an ideal droplet:*

$$\mathcal{J}^{i+1}(\mathbf{u}, E) = \frac{1}{2}\|\mathbf{X}^{i+1}(0)(\cdot) + \delta t\mathbf{u}(\cdot) - \mathbf{X}_d^{i+1}(\cdot)\|^2_{L^2(\Gamma^i)} + \frac{\zeta}{2}\|E\|^2_{\mathcal{E}}.$$

   Here, $\mathbf{X}_d^{i+1}(\cdot)$ is a closed curve in $\mathbb{R}^2$ that represents a desired droplet shape at time i, whereas $\mathbf{X}^{i+1}(0)(\cdot)$ is the identity map on the boundary Γ^i, as defined in the introduction. More specifically, we assume that $\mathbf{X}^{i+1}(0) := \Gamma^i$ and $\mathbf{X}_d^{i+1}$ have parametrizations of the form $(x_1(s), x_2(s))$ and $(x_1^d(s), x_2^d(s))$ $s \in [0, 1]$, respectively, and we consider the first term in the objective as follows:

$$\frac{1}{2}\sum_{j=1}^{2}\int_0^1 \Big(x_j(s) + \delta t_{i+1}\big(\mathbf{u} \circ (x_1, x_2)\big)(s) \cdot \mathbf{e}_j - x_j^d(s)\Big)^2 ds,$$

   where $\mathbf{e}_1, \mathbf{e}_2$ are the standard basis vectors of $\mathbb{R}^2$. In our experiments, we set $\mathbf{X}_d^{i+1} := \mathbf{X}_d$, where $\mathbf{X}_d$ is some ideal droplet shape.
4. *Minimal velocity and barycenter matching:*

$$\mathcal{J}^{i+1}(\mathbf{u}, E) = \frac{1}{2}\|\mathbf{u}(\cdot)\|^2_{L^2(\Gamma^i)} + \frac{1}{2}\left\| \frac{1}{|\Omega^i|}\int_{\Omega^i} \big(x + \delta t_{i+1}\mathbf{u}(x)\big)\, dx - \mathbf{b}_d \right\|^2_{\mathbb{R}^2} + \frac{\zeta}{2}\|E\|^2_{\mathcal{E}}.$$

   Given an ideal droplet shape $\mathbf{X}_d^{i+1}(\cdot)$ with barycenter $\mathbf{b}_d$, the first term in $\mathcal{J}^{i+1}$ enforces a minimal velocity (stationary configuration). The second term positions the droplet at a desired location by enforcing barycenter matching.

The barycenter functionals have the advantage of not relying on information concerning the shape of the droplet. For droplets that are slightly larger than the size of the individual electrodes on the surface of the EWOD device, these are useful objectives. Indeed, here the effect of the surface tension on the droplet should somewhat inhibit topological changes. However, for droplets whose

"footprint", i.e., support within $\mathbb{R}^2$, is much larger than the size of an electrode they might not be ideal objectives, cf. [51].

The tracking-type objective, on the other hand, relies on information concerning the current and the next free boundary. It is theoretically more challenging and it requires us to provide substantial information on the ideal trajectory of a droplet. However, by providing the path of a droplet whose topology does not change over the time interval, it is possible to obtain a sequences of controls that keep the original droplet's topology intact.

Note that the functional in 3 forces a parametrization of the surface. If instead, we could work with the characteristic functions associated with the droplet footprints, then we might be able to track a sequence of "ideal" footprints. Here, we would consider the minimization of the distance between the associated characteristic functions at each time step. This would be similar to the approach in [38]. However, it appears that one would need a shape sensitivity analysis to do so, which goes beyond the scope of this paper due to the presence of a variational inequality. We refer to the related work with a simpler forward problem [28].

4.2 *The control action and* $\mathfrak{E}_{ad}$

We need to take into consideration the physical limitations of the EWOD device and realistic opportunities for the control action. Based on our theory, it is possible to consider finite dimensional or distributed controls. We propose the following setting: Given a square, 3×3 EWOD device, we define 9 domains Ω_j, $j = 1, \dots, 9$ and 9 controls/control spaces $E_j^i \in \mathfrak{E}_j^i$. The linear operator F_0 and the theoretical results can be easily adapted to this setting. Before, we used:

$$\langle F_0^i(E^i), \mathbf{v} \rangle := -(E^i, \mathbf{v} \cdot \boldsymbol{\nu}^i)_{L^2(\Gamma^i)}.$$

Alternatively, we could use at the i^{th} time step:

$$\left\langle F_0^i(E_1^i, \dots, E_9^i), \mathbf{v} \right\rangle := -\sum_{j=1}^{9} \int_{\Gamma^i \cap \Omega_j} E_j^i \mathbf{v} \cdot \boldsymbol{\nu}^i \, ds.$$

Since a distributed control may not be physically realizable, we consider a finite dimensional setting in which $\mathfrak{E}_j^i = \mathbb{R}$. We then have

$$\left\langle F_0^i(E_1^i, \dots, E_9^i), \mathbf{v} \right\rangle := -\sum_{j=1}^{9} E_j^i \int_{\Gamma^i \cap \Omega_j} \mathbf{v} \cdot \boldsymbol{\nu}^i \, ds.$$

This new choice of F_0 would affect the concrete realization of (3.10); we discuss this below in the calculation of an update in the control procedure.

In our setting, we control the contact angle on the free boundary via E, the EWOD forcing term. Given E, one can obtain the needed voltage for a specific electrode provided empirical data is available, which relate the contact angle to the applied voltage. Indeed, the vertical curvature component of the Laplace pressure on the interface is given by $\kappa_z = -\left[\cos(\theta_{\text{top}}) + \cos(\theta_{\text{bot}})\right]$ on Γ, where θ_{top} and θ_{bot} represent the upper and lower contact angles, respectively. For our experiments, we set $\theta_{\text{top}} := 90°$ and assume that θ_{bot} is directly related to the underlying voltage V applied to the associated electrode, i.e., we may consider κ_z as a function of V at point x. After rescaling κ,

one sets $E(x) := c\kappa_z(V(x)) = -c\left[\cos(\theta_{\text{top}}) + \cos(\theta_{\text{bot}}(V(x)))\right]$, where $c > 0$ is related to the attributes of the EWOD device. For more, we refer the reader to the discussion surrounding [51, Eqs. (6) and (8)].

Following [51], we consider the control of a Glycerin droplet. The contact angle θ_{bot}, along with all other material constants, e.g., α, β, are provided in [51, Table II]. For instance, when $V = 0\,\text{V}$, θ_{bot} is 107.35° and when $V = 50\,\text{V}$ the θ_{bot} is 68.46°. These contact angles (neglecting the top contact angle) combined with the empirical relation between the contact angle and E provide us with the box constraints on the control E, i.e.,

$$\mathcal{E}_{ad} = \left\{E \in L^2(\Gamma) : -11.0145 \leqslant E(s) \leqslant 8.9462, \text{ a.e. } s \in \Gamma\right\}.$$

These contact bounds are easily applied in the finite dimensional case as well. Note that in the distributed case, i.e., when $E \in \mathcal{E}_{ad} \subset L^2(\Gamma)$, we have the usual pointwise almost-everywhere projection formula.

4.3 *Solving the forward system*

At each step of the algorithm, we need an efficient solver of the smoothed EWOD problem in solenoidal form:

$$A\mathbf{u} + C^*\Psi'_\alpha(C\mathbf{u}) = F(E).$$

Since we operate under the setting of [48, 51], where the authors use P2-P1 elements, which are not divergence free, in general we revert to the non-solenoidal system.

In light of these aspects, we revert to the non-solenoidal system:

$$A\mathbf{u} + B^*p + P_{\text{pin}}C^*\lambda = F(E), \tag{4.1a}$$

$$B\mathbf{u} = 0, \tag{4.1b}$$

$$\lambda = \Psi'_\alpha(C\mathbf{u}). \tag{4.1c}$$

Here, (4.1c) is be understood for pointwise almost every $s \in \Gamma$ as

$$\lambda(s) = \widetilde{\psi}'\big(\alpha^{-1}(C\mathbf{u})(s)\big).$$

For our numerical experiments, we suggest the following (convex C^2) form for $\widetilde{\psi}$ (see Figure 1): For $r \in \mathbb{R}$, we have

$$\widetilde{\psi}(r) := \begin{cases} r - 1/2, & r \geqslant 1, \\ r^3 - r^4/2, & r \in (0,1), \\ -r^3 - r^4/2, & r \in (-1,0], \\ -r - 1/2, & r \leqslant -1. \end{cases} \qquad \widetilde{\psi}'(r) = \begin{cases} 1, & r \geqslant 1, \\ 3r^2 - 2r^3, & r \in (0,1), \\ -3r^2 - 2r^3, & r \in (-1,0], \\ -1, & r \leqslant -1. \end{cases}$$

In addition, we have

$$\widetilde{\psi}''(r) = \begin{cases} 0, & r \geqslant 1, \quad \text{or} \quad r \leqslant -1, \\ 6(r - r^2), & r \in (0,1), \\ -6(r + r^2), & r \in (-1,0]. \end{cases}$$

As stated earlier, see the discussion following (3.3), the smoothing of ψ, i.e., the absolute value, induces (perhaps) non-physical pinning, see Section 4.6. In light of our choice of $\widetilde{\psi}$ above, this type

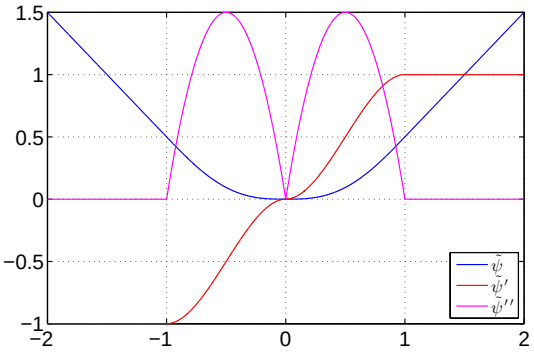

FIG. 1. The panel shows $\widetilde{\psi}$, $\widetilde{\psi}'$, and $\widetilde{\psi}''$.

of slipping is confined to the small interval $(-\alpha, \alpha)$; recall that $\alpha \downarrow 0$. Note also that the sufficient conditions in Proposition 5.1 for the differentiability of the induced superposition/Nemytski operator are satisfied.

In order to solve (4.1), we use an exact solver and we resort to a regularization approach by adding a small amount of compressibility, i.e., the perturbation εp, to the left side of (4.1b). Alternatively, we could use an iterative scheme such as Uzawa. For each fixed $\alpha > 0$ and $\varepsilon > 0$, we can the solve the resulting system with the standard Newton's method with a simple backtracking line search as a globalization scheme. The stopping criteria was based on the discrete $\mathbb{V}$-norm of the Riesz representation in $\mathbb{V}$ of the residual of the system (4.1) with an absolute tolerance of $1e$-10; ε was set to $1e$-16. The method exhibited fast/superlinear convergence, e.g., averaging 3–4 iterations until convergence, throughout the experiments. The performance was slightly worsened for cases involving large deformations of the droplet.

The algorithm has been implemented in MATLAB; extensive use was made of the software library FELICITY [47]. As suggested in [48], we discretized the problem using $\mathcal{P}_2 - \mathcal{P}_1$-Taylor–Hood finite elements, see, e.g., [14]. Moreover, in order to ensure a geometrically consistent discretization of the droplet and proper computation of the curvature, cf. [5], piecewise quadratic isoparametric elements were employed on those elements that contained a portion of the boundary Γ. Finally, we note that the matrices for the linear systems of equations (in both the Newton iteration as well as the solution of the adjoint equation) are assembled using a numerical quadrature formula that is exact for polynomials up to degree 12.

After each time step, the mesh may become severely distorted or thin neck regions may appear. We follow [51, III.F.2] in order to partially circumvent these issues. In particular, a so-called harmonic lifting is applied in which the current velocity $\mathbf{u}|_\Gamma$ is used as the boundary data for a harmonic equation. This yields a vector field that smoothly updates the mesh node positions at each time step and preserves the shape of the boundary. In case of significantly large deformations, a further remedy is suggested in [51, III.F.3]; this was not employed/needed in our experiments.

4.4 *Additional aspects of the forward system: Updating α*

Since we are considering the smoothed EWOD system, any sequence of controls that we generate will implicitly depend on α. Inspired by [25, 26] and considering α to induce a primal-dual path

$\mathcal{P} := \{(\mathbf{u}_\alpha, p_\alpha, \lambda_\alpha) \,|\alpha > 0\}$, one would ultimately hope to have an analytical path-following scheme that leads to a proper update strategy for α. Unfortunately, the structure of (4.1) rules out an immediate application of [25, 26]. As a fully automated and sensitivity-based path-following scheme for (4.1) clearly goes beyond the scope of the present work, we resort to a "manual" update strategy for α. In this context, it is also important to decide *when* to update α along the time steps. Since we apply an instantaneous control strategy, it is important that the controls on each time interval are related to the same forward system (which depends on α); the only difference between the system at t_{i+1} and t_i are the inputs used at t_{i+1}, e.g., $(\mathbf{u}^i, \Gamma^i)$ obtained at t_i. Therefore, we invoke a gradual reduction scheme for α at t_1 in order to reach a sufficiently close approximation of the original pinning relation. Afterwards, we keep α fixed for all subsequent time intervals. In our experiments, α was initialized at $1e$-2 and reduced to the order of $1e$-6. Smaller initial values, e.g., $1e$-3, led to failure of the Newton solver. Finally, we mention that a time step of size $1e$-3 was employed; larger time steps typically led to larger mesh deformations and failure of Newton's method.

4.5 *Updating the control at time t_i*

Supposing that we are again in the 3×3 EWOD regime, let $E^i_{j,k}$, $j \in \{1, \dots, 9\}$, be the k^{th} iterate of the j^{th} control at time t_i. Substituting $(E^i_{1,k}, \dots, E^i_{9,k})$ into (4.1) and solving as described above, we obtain $\mathbf{u}^i_k$, the k^{th} iterate of the velocity field at time t_i. Given $\mathbf{u}^i_k$, we calculate $\partial_E \mathcal{J}_\alpha(E^i_{1,k}, \dots, E^i_{9,k})$ and update the controls.

Ignoring the box constraints $\mathcal{E}_{ad}$, (3.6) yields the preliminary update:

$$\partial_{E_j} \mathcal{J}_\alpha(E^i_{1,k}, \dots, E^i_{9,k}) = \zeta E^i_{j,k} - \int_{\Gamma_i \cap \Omega_j} \mathbf{w}^i_k \cdot \boldsymbol{\nu} ds, \;\; j \in \{1, \dots, 9\}, \tag{4.2}$$

where $\mathbf{w}^i_k$ is the k^{th} iterate of the adjoint state obtained by solving the saddle point problem

$$\big[A + P_{\text{pin}} C^* \Psi''_\alpha(C\mathbf{u}_\alpha) C\big]\mathbf{w} + B^* q = -\partial_{\mathbf{u}} \widehat{\mathcal{J}}(E^i_{1,k}, \cdots, E^i_{9,k}, \mathbf{u}^i_k), \tag{4.3a}$$

$$B\mathbf{w} = 0. \tag{4.3b}$$

Finally, we update the control using a projected BFGS strategy as suggested in [36] until either the $\mathbb{R}^9$ norm of the residual $E_k - \text{Proj}_{\mathcal{E}_{ad}}(E_k - \nabla \mathcal{J}_\alpha(E_k))$ was below $1e$-10 or 15 iterations were reached. We experimentally selected 15, as the solutions appeared to be sufficiently accurate.

4.6 *Forward solver results*

To study the affect of regularization α we first design a semismooth Newton solver for our nonsmooth forward problem (2.1). Notice that no regularization appears in the semismooth Newton. Subsequently we compare the semismooth Newton results when applied to (2.1) with the Newton results when applied to (4.1). These results are shown in Figure 2. We further remark that, qualitatively, our results for this experiment matches with [51].

4.7 *Optimization results*

In this subsection, we present the results of the method as applied to four examples, one for each objective functional. We set $T = 3s$ and $\delta t = 1e$-3, the initial droplet is a circle of diameter

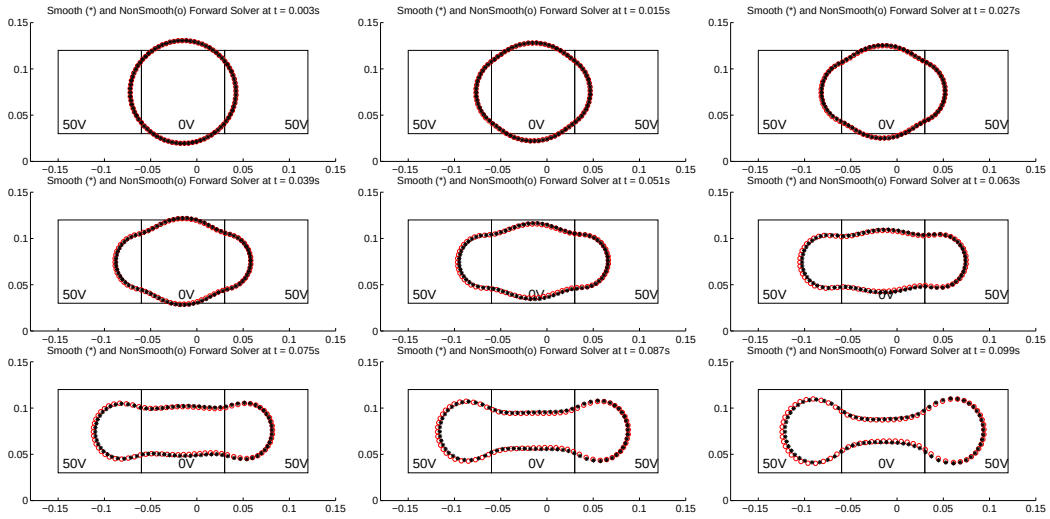

FIG. 2. We solve the regularized problem (4.1) and the nonsmooth problem (2.1) by using Newton and semismooth Newton, respectively. Notice that no regularization is needed in the semismooth Newton. The panels show comparison between the two approaches at different time instances.

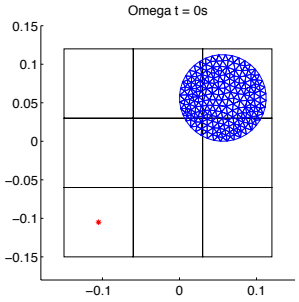

FIG. 3. Initial configuration for barycenter matching: Initial droplet (top right) and desired barycenter (bottom left).

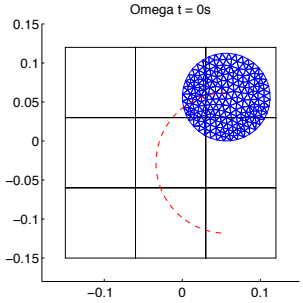

FIG. 4. Initial configuration for barycenter tracking: Initial droplet (top right) and desired trajectory (dotted semicircle).

0.1125 mm and is centered at $(0.05625, 0.05625)$ mm. As discussed above, we consider an EWOD device with 3×3 configuration of electrodes. For each of the experiments, we provide the behavior of the droplets over nine points in time; refer to the figures below. The values of the nine separate controls are printed inside their respective electrodes at those points in time. Recall as mentioned above, that $E = 8.9462$ corresponds to 0 V and $E = -11.0145$ to 50 V.

1. *Barycenter matching:* For this example, we set the desired barycenter $\mathbf{b}_d = (-0.105, -0.105)$. The results of this experiment can be seen in Figures 5. In Figure 6 we show the behavior of line search at a particular time instance.

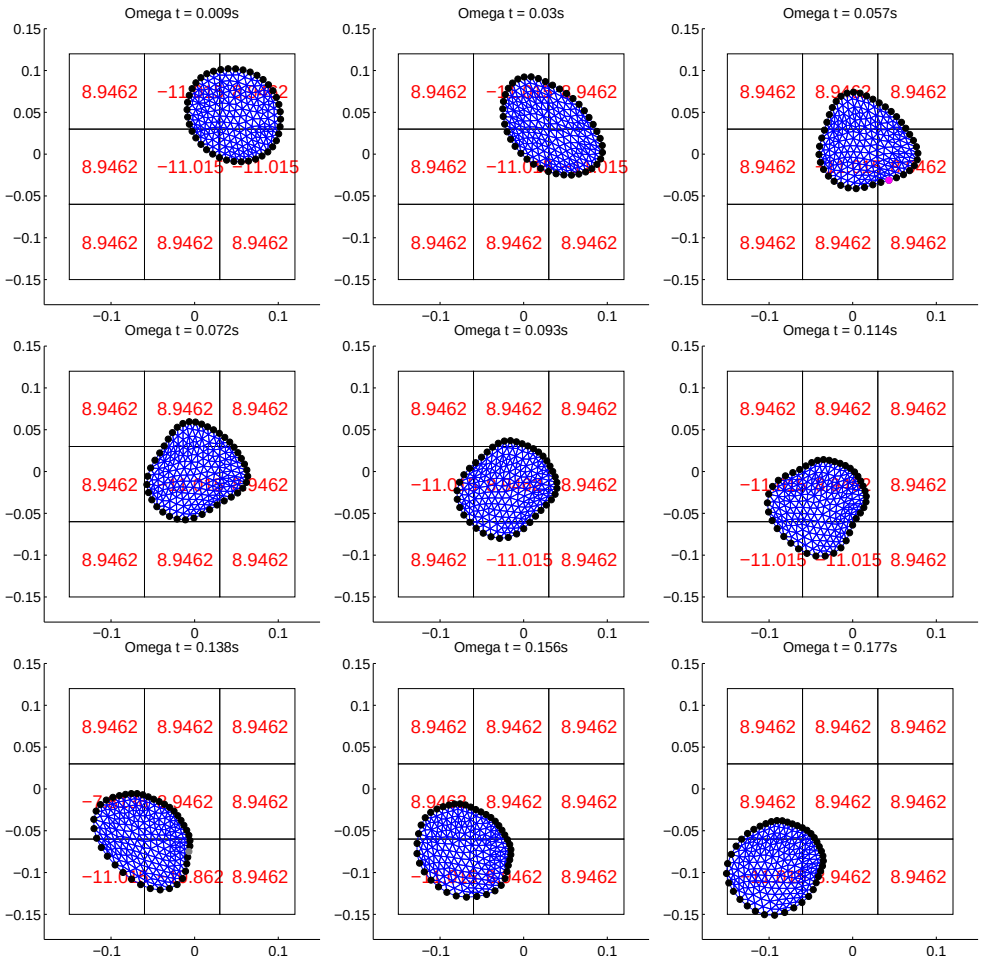

FIG. 5. Barycenter matching: The 9 panels show the mesh modification at different times (in sec). The control E, shown in the background, is piecewise constant on each electrode. $E = 8.9462$ implies that a voltage of 0 V is applied to that electrode and $E = -11.015$ correspond to 50 V. The active/inactive sets on the boundary are denoted by **Black** •: strongly active, Magenta • [online version]: biactive, Grey •: inactive. Note the biactivity at time $t = 0.057$ s.

2. *Barycenter tracking:* Here, the ideal barycenters follow the semicircle starting at $(0.05625, 0.05625)$ and following the path described by $\mathbf{b}_d(t)$ where $\mathbf{b}_d(t) := (\mathbf{b}_{d,1}(t), \mathbf{b}_{d,2}(t))$ is given by

$$\mathbf{b}_{d,1}(t) = 0.09\cos\big(\phi(t)\big) + 0.05625, \quad \mathbf{b}_{d,2}(t) = 0.09\sin\big(\phi(t)\big) - 0.02813$$

with $\phi(t) := (3-t)\pi/6 + t\pi/2$, $t \in [0,3]$; compare Figures 3 and 4. We let $t_0 = 0$ and $t_K = T$ in our experiments. The results of this experiment can be seen in Figure 7

3. *Matching the shape of an ideal droplet:* In this example the ideal droplet is taken to be $\mathbf{X}^{i+1}(0)(\cdot) - 0.1350$. The initial droplet is as in the previous two examples. The results of this experiment can be seen in Figure 8.

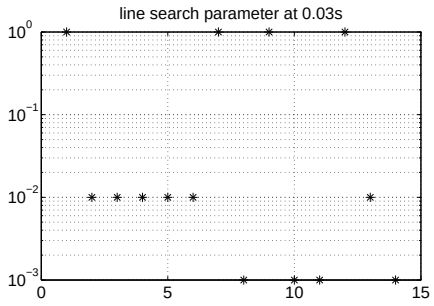

FIG. 6. The panel shows the line search parameter (y-axis) with optimization iterate on x-axis at $t = 0.03$ s.

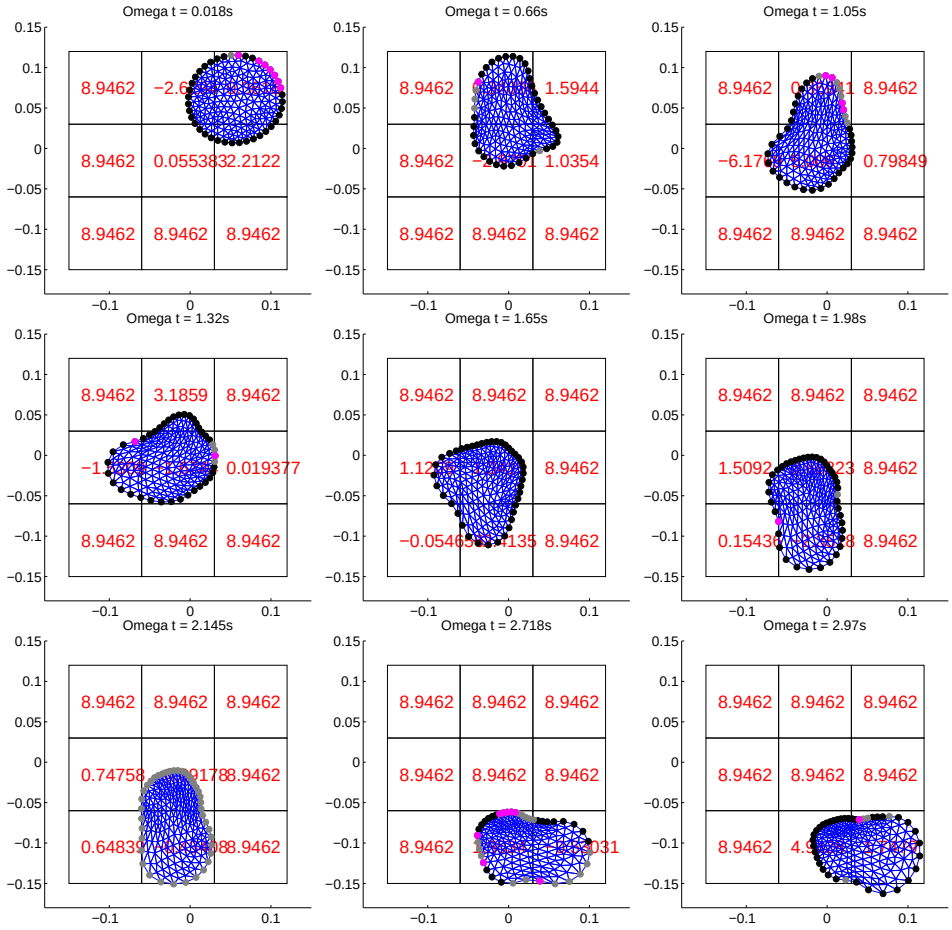

FIG. 7. Barycenter tracking: The 9 panels show the mesh modification at different times (in sec). The control E, shown in the background, is piecewise constant on each electrode. $E = 8.9462$ implies that a voltage of 0 V is applied to that electrode and $E = -11.015$ correspond to 50 V. The active/inactive sets on the boundary are denoted by **Black** •: strongly active, Magenta • [online version]: biactive, Grey •: inactive. Note the biactivity at times $t = 0.018$ s, 0.66 s, 1.05 s, 1.32 s, 1.98 s, 2.718 s, 2.97 s.

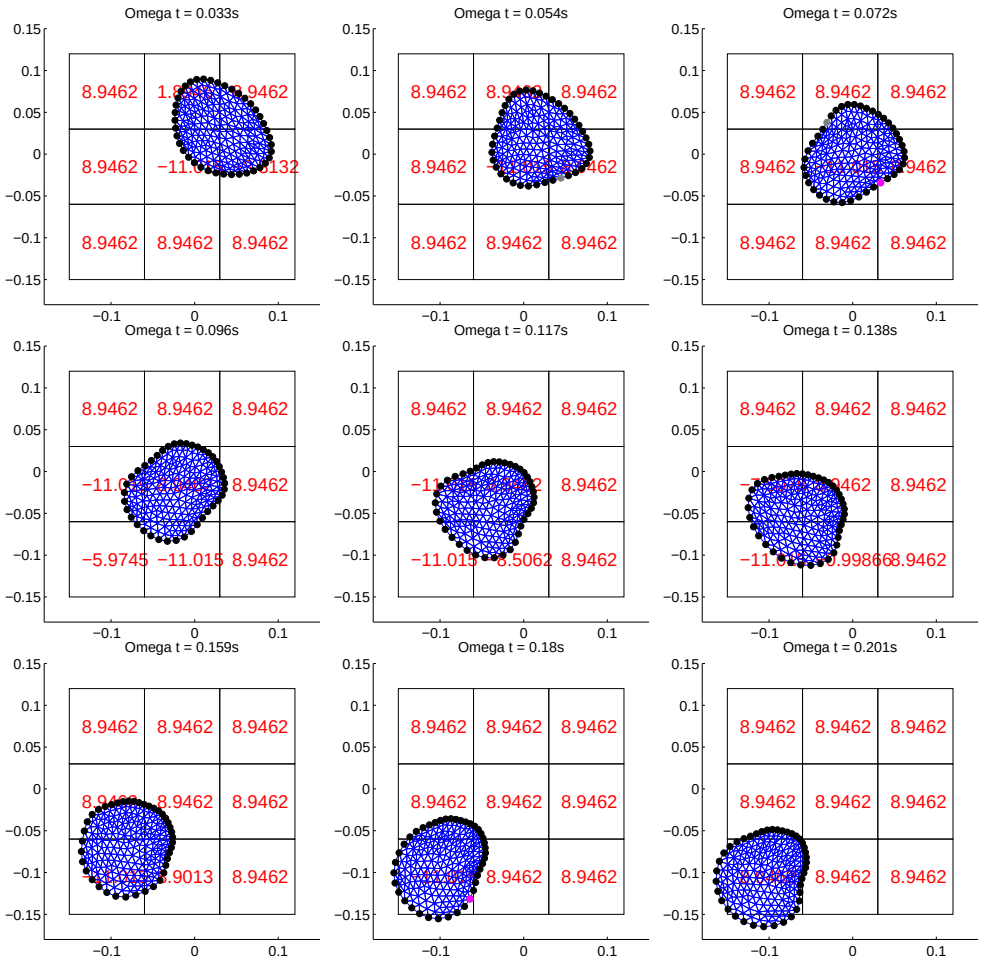

FIG. 8. Matching an Ideal Droplet: The 9 panels show the mesh modification at different times (in sec). The control E, shown in the background, is piecewise constant on each electrode. $E = 8.9462$ implies that a voltage of 0 V is applied to that electrode and $E = -11.015$ correspond to 50 V. The active/inactive sets on the boundary are denoted by **Black** •: strongly active, Magenta • [online version]: biactive, Grey •: inactive. Note the biactivity at times $t = 0.072$ s.

4. *Minimal velocity and barycenter matching:* The initial droplet is an ellipse (•) and the ideal (desired) droplet is a circle (○) of the same size as in Figure 3. Furthermore to increase the impact of the controls we have reduced the size of electrodes by half. The results of this experiment can be seen in Figure 9.

5. Conclusions and future directions

In this paper, we considered the finite horizon model predictive control of a time-discrete model of electrowetting on dielectric (EWOD) in which the effects of molecular adhesion and contact line hysteresis are modeled by a subdifferential inclusion/complementarity relation. Due to the difficulty

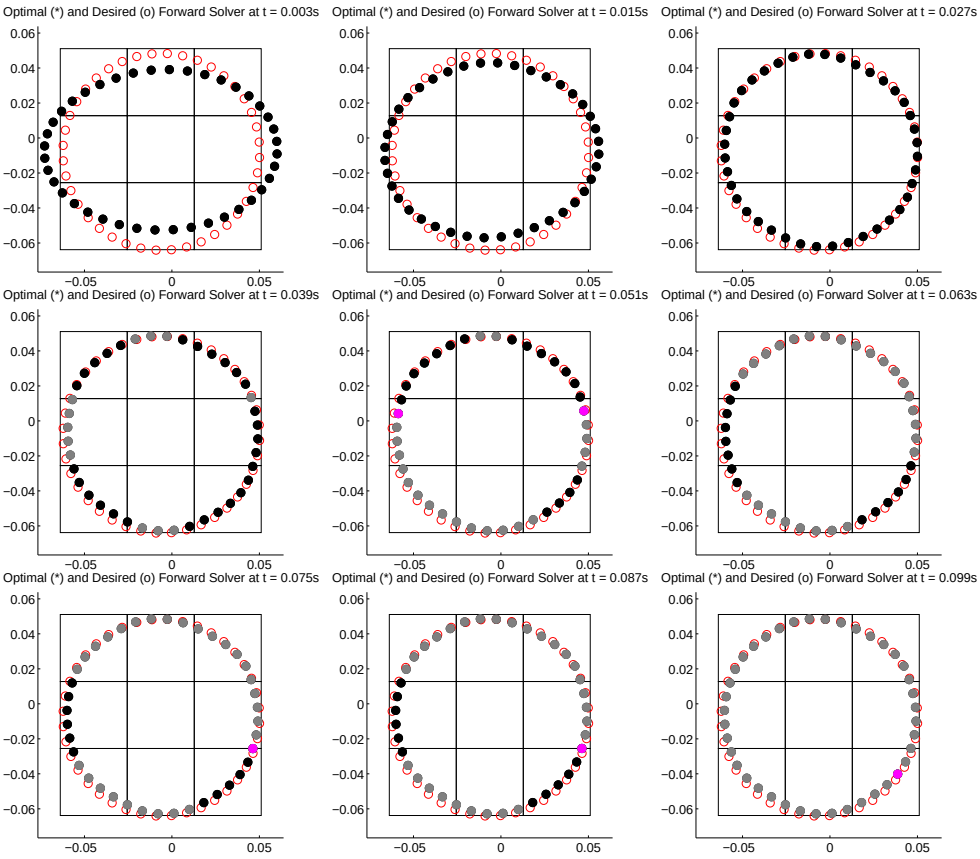

FIG. 9. Minimal velocity and Barycenter Matching: The 9 panels show the optimal shape (●) and the desired shape (○) at different times (in sec). The active/inactive sets on the boundary are denoted by **Black** ●: strongly active, Magenta ● [online version]: biactive, Grey ●: inactive.

of including the free boundary (a non-implicit, non-graph form geometric variable) as a decision variable, a comprehensive optimal control approach in which the coupled EWOD systems as well as the evolution of the free boundary appear in the constraint set was ruled out. This led us to consider a model predictive control approach, which, in each time interval, requires the solution of an optimization problem with a variational inequality constraint, i.e., an elliptic mathematical program with equilibrium constraints (MPEC). Due to the difficult nature of elliptic MPECs, a smoothing approach was considered for the derivation of optimality conditions at each time step. These conditions may serve as stopping criteria for an associated numerical method. Moreover, the smoothing approach provides us with a means of calculating a sequence of controls that correspond to the voltages applied to the electrodes in an EWOD device. In our numerical experiments, we considered a model EWOD device with a 3×3 electrode configuration and the movement of a droplet of glycerin. In particular, we demonstrated how the general theoretical and numerical approach can be applied to the cases of barycenter matching and tracking as well as the matching of an ideal droplet shape. Moreover, especially in the case of barycenter tracking, we noted the

persistent presence of biactivity throughout the time steps. Thus, we have considered examples where the control-to-state mapping is truly non-smooth. Finally, concerning the choice of finite element discretization of the smooth or non-smooth EWOD system, we also refer to [15], where the authors develop divergence-free elements to study an EWOD system. However, the authors do not account for pinning. The extension to pinning and subsequently control will be the focus of future work.

Appendix

In the following technical result, we specify a class of functionals Ψ_α that satisfies (i)–(v) (at the beginning of Section 3.2). The conditions are inspired by those found in, e.g., [7].

Proposition 5.1 *Let $\{\varepsilon_\alpha\}_{\alpha>0}$ be a sequence in $\mathbb{R}$ such that $\varepsilon_\alpha \to 0$ as $\alpha \downarrow 0$, $1 \geqslant |\varepsilon_\alpha|$, and let $\widetilde{\psi} : \mathbb{R} \to \mathbb{R}$ be convex and twice continuously differentiable such that:*

1. *For all $r \in \mathbb{R}$, $\widetilde{\psi}(r) \geqslant \psi(r) = |r|$,*
2. *For all $r \in \mathbb{R}$, $\widetilde{\psi}''(r) < c$, for some constant $c \in \mathbb{R}$,*
3. *The following two conditions hold:*

$$\lim_{r\to-\infty} r^{-1}\big(\widetilde{\psi}(r)\big) = -1, \quad \lim_{r\to+\infty} r^{-1}\big(\widetilde{\psi}(r)\big) = +1. \tag{5.1}$$

Then, defining $\psi_\alpha : \mathbb{R} \to \mathbb{R}$ (a regularization of ψ) by $\psi_\alpha(r) := \alpha\widetilde{\psi}(\alpha^{-1}r) + \varepsilon_\alpha$, the family of functionals $\{\Psi_\alpha\}_{\alpha>0}$ given by

$$\Psi_\alpha(v) := \int_\Gamma \psi_\alpha\big(v(s)\big)ds, \quad v \in L^2(\Gamma),$$

together with $\Psi(v) := \int_\Gamma \psi\big(v(s)\big)ds$, satisfies the conditions (i)–(v).

Proof. We first note that (5.1) implies

$$\frac{r\widetilde{\psi}(s)}{s} \to r, \text{if } r > 0, s \to +\infty; \quad \frac{r\widetilde{\psi}(s)}{s} \to -r, \text{if } r < 0, s \to -\infty; \quad \frac{r\widetilde{\psi}(s)}{s} \to 0, \text{else.}$$

Hence, $rs^{-1}\widetilde{\psi}(s) \to |r|$ provided r and s have the same sign, or $r = 0$. Consequently, we have

$$\lim_{\alpha\downarrow 0} \psi_\alpha(r) = \lim_{\alpha\downarrow 0} \alpha\widetilde{\psi}(\alpha^{-1}r) = |r| = \psi(r). \tag{5.2}$$

We now prove (i)–(v).

(i) Since $\widetilde{\psi}''$ is bounded on $\mathbb{R}$, the corresponding superposition (Nemytski) operator maps $L^p(\Gamma)$ continuously to $L^\infty(\Gamma)$. Consequently, the superposition operator associated with $\widetilde{\psi}'$ is continuously Frèchet differentiable from $L^p(\Gamma)$ into $L^{p'}(\Gamma)$, cf. [3, 17]. This property then transfers to Ψ'_α.

(ii) Given $\psi_\alpha(r) \geqslant \varepsilon_\alpha$ and $\{\varepsilon_\alpha\}$ is bounded, (ii) follows immediately.

(iii) Let $u \in L^2(\Gamma)$. By our assumptions, it holds that $0 \leqslant \psi_\alpha(u(s)) \leqslant \psi_1(u(s)) + 1$ for almost every $s \in \Gamma$ and for all $\alpha \in (0, 1]$. Since $\psi_\alpha(\cdot)$ is continuous, $f_\alpha(\cdot) := \psi_\alpha(u(\cdot))$ is measurable. Finally, we see that f_α converges pointwise almost everywhere to $\psi(u(s))$ as $\alpha \downarrow 0$. Combining these properties we see that $f_\alpha \to \psi \circ u$ strongly in $L^1(\Gamma)$ by Lebesgue's dominated convergence theorem.

(iv) Fixing once again $u \in L^2(\Gamma)$, let $\alpha \downarrow 0$ and $u_\alpha \rightharpoonup u$ in $L^2(\Gamma)$. Since $\alpha\widetilde{\psi}(\alpha^{-1}r) \geqslant \alpha\psi(\alpha^{-1}r) = \psi(r)$ we have that

$$\begin{aligned}\liminf_{\alpha\to 0} \Psi_\alpha(u_\alpha) &= \liminf_{\alpha\downarrow 0} \int_\Gamma \alpha\widetilde{\psi}\big(\alpha^{-1}u_\alpha(s)\big)\,ds \geqslant \liminf_{\alpha\downarrow 0} \int_\Gamma \psi\big(u_\alpha(s)\big)\,ds \\ &= \liminf_{\alpha\to 0} \Psi(u_\alpha) \geqslant \Psi(u),\end{aligned}$$

by the weak lower-semicontinuity of Ψ. This shows (iv).

(v) Due to convexity and differentiability, $\Psi'_\alpha(\cdot)$ is monotone. Then for any bounded subset $\mathfrak{M} \subset \mathbb{V}^*_{\mathrm{sol}}$, $\alpha > 0$, and $\mathbf{u} \in \mathbb{V}_{\mathrm{sol}}$ that satisfies $A\mathbf{u} + C^*\Psi'_\alpha(C\mathbf{u}) = f \in \mathfrak{M}$, we get

$$\begin{aligned}\epsilon\|\mathbf{u}\|^2_{\mathbb{V}} &\leqslant \big\langle A\mathbf{u} + C^*\Psi'_\alpha(C\mathbf{u}) - \big(A(0) + C^*\Psi'_\alpha(0)\big), \mathbf{u} - 0\big\rangle \\ &= \langle f - C^*\Psi'_\alpha(0), \mathbf{u}\rangle \\ &\leqslant \sup_{f\in\mathfrak{M}} (\|f\|_{\mathbb{V}^*_{\mathrm{sol}}} + \epsilon')\|\mathbf{u}\|_{\mathbb{V}} \leqslant \epsilon''\|\mathbf{u}\|_{\mathbb{V}}, \quad (5.3)\end{aligned}$$

where $\epsilon > 0$ is the ellipticity constant of A and the constants $\epsilon', \epsilon'' > 0$ are the result of embeddings and the boundedness of $\mathfrak{M}$.

This completes the proof. □

Acknowledgments. The authors gratefully acknowledge the helpful support by the DFG Grant to Support the Initiation of International Collaboration HI 1466/5-1. We would also like to thank Shawn Walker for his many helpful tips and comments, especially concerning the usage of FELICITY. M.H., D.W. acknowledge the support by DFG-SPP 1506 grant HI 1466/2-1. M.H., T.M.S., D.W. acknowledge the support by the Research Center MATHEON through the Project C-SE5 through the Einstein Center for Mathematics Berlin as well as the DFG Grant to Support the Initiation of International Collaboration HI 1466/5-1. H.A. acknowledges the support by the NSF-DMS-1521590 and the DFG Grant to Support the Initiation of International Collaboration HI 1466/5-1. R.H.N. acknowledges the support by NSF Grant DMS-1411808 and the DFG Grant to Support the Initiation of International Collaboration HI 1466/5-1.

References

1. Antil, H., Nochetto, R. & Sodré, P., Optimal control of a free boundary problem with surface tension effects: A priori error analysis. *SIAM J. Numer. Anal.* **53** (2015), 2279–2306. Zbl1343.49043 MR3404685
2. Antil, H., Nochetto, R. H. & Sodré, P., Optimal control of a free boundary problem: Analysis with second-order sufficient conditions. *SIAM J. Control Optim.* **52** (2014), 2771–2799. Zbl1311.49008 MR3256797
3. Appell, J. & Zabrejko, P. P., *Nonlinear Superposition Operators*, vol. 95 of *Cambridge Tracts in Mathematics*. Cambridge University Press, Cambridge, 1990. Zbl0701.47041 MR1066204
4. Barbu, V., *Optimal Control of Variational Inequalities*, vol. 100 of *Research Notes in Mathematics*. Pitman (Advanced Publishing Program), Boston, MA, 1984. Zbl0574.49005 MR0742624
5. Bonito, A., Nochetto, R. H. & Pauletti, M. S., Geometrically consistent mesh modification. *SIAM J. Numer. Anal.* **48** (2010), 1877–1899. Zbl1220.65169 MR2733102
6. Browder, F. E., Nonlinear variational inequalities and maximal monotone mappings in Banach spaces. *Math. Ann.* **183** (1969), 213–231. Zbl0208.39105 MR0271780

7. Chen, C. H. & Mangasarian, O. L., Smoothing methods for convex inequalities and linear complementarity problems. *Math. Programming* **71** 1, Ser. A (1995), 51–69. Zbl0855.90124 MR1362957
8. Cho, S. K. & Kim, C.-J., Particle separation and concentration control for digital microfluidic systems. In *Micro Electro Mechanical Systems, 2003. MEMS-03 Kyoto. IEEE The Sixteenth Annual International Conference on* (Jan 2003), pp. 686–689.
9. Cho, S. K., Moon, H. & Kim, C.-J., Creating, transporting, cutting, and merging liquid droplets by electrowetting-based actuation for digital microfluidic circuits. *J. Microelectromech. S.* **12** (2003), 70–80.
10. Croft, W., Elliott, C. M., Ladds, G., Stinner, B., Venkataraman, C. & Weston, C., Parameter identification problems in the modelling of cell motility. *J. Math. Biol.* **71** (2015), 399–436. Zbl1321.92043 MR3367680
11. De Los Reyes, J. C., Optimal control of a class of variational inequalities of the second kind. *SIAM J. Control Optim.* **49** (2011), 1629–1658. Zbl1226.49008 MR2837569
12. Deckelnick, K., Elliott, C. M. & Styles, V., Optimal control of the propagation of a graph in inhomogeneous media. *SIAM J. Control Optim.* **48** (2009), 1335–1352. Zbl1282.49003 MR2496979
13. Delfour, M. C. & Zolésio, J.-P., *Shapes and Geometries*, second ed., vol. 22 of *Advances in Design and Control*. Society for Industrial and Applied Mathematics (SIAM), Philadelphia, PA, 2011. Metrics, analysis, differential calculus, and optimization. Zbl1251.49001 MR2731611
14. Ern, A. & Guermond, J.-L., *Theory and Practice of Finite Elements*, vol. 159 of *Applied Mathematical Sciences*. Springer-Verlag, New York, 2004. Zbl1059.65103 MR2050138
15. Falk, R. S. & Walker, S. W., A mixed finite element method for EWOD that directly computes the position of the moving interface. *SIAM J. Numer. Anal.* **51** (2013), 1016–1040. Zbl1268.76063 MR3035483
16. Garcia, C. E., Prett, D. M. & Morari, M., Model predictive control: Theory and practice – a survey. *Automatica* **25** (1989), 335–348. Zbl0685.93029
17. Goldberg, H., Kampowsky, W. & Tröltzsch, F., On Nemytskij operators in L_p-spaces of abstract functions. *Math. Nachr.* **155** (1992), 127–140. Zbl0760.47031 MR1231260
18. Gong, J., Fan, S.-K. & Kim, C., Portable digital microfluidics platform with active but disposable lab-on-chip. In *Micro Electro Mechanical Systems, 2004. 17th IEEE International Conference on. (MEMS)* (2004), pp. 355–358.
19. Haslinger, J., Stebel, J., & Sassi, T. Shape optimization for Stokes problem with threshold slip. *Applications of Mathematics* **59** (2014), 631–652. Zbl1340.49043 MR3277731
20. Heikenfeld, J., Zhou, K., Kreit, E., Raj, B., Yang, S., Sun, B., Milarcik, A., Clapp, L. & Schwartz, R., Electrofluidic displays using Young-Laplace transposition of brilliant pigment dispersions. *Nat Photon* **3** (2009), 292–296.
21. Herzog, R., Meyer, C. & Wachsmuth, G., B- and strong stationarity for optimal control of static plasticity with hardening. *SIAM J. Optim.* **23** (2013), 321–352. Zbl1266.49013 MR3033110
22. Hintermüller, M., Keil, T. & Wegner, D., Optimal control of a semidiscrete Cahn–Hilliard–Navier-Stokes system with non-matched fluid densities. To appear in *SIAM J. Control Optim.*
23. Hintermüller, M. & Kopacka, I., Mathematical programs with complementarity constraints in function space: C- and strong stationarity and a path-following algorithm. *SIAM J. Optim.* **20** (2009), 868–902.
24. Hintermüller, M. & Kopacka, I., A smooth penalty approach and a nonlinear multigrid algorithm for elliptic MPECs. *Comput. Optim. Appl.* **50** (2011), 111–145. Zbl1229.49032 MR2822818
25. Hintermüller, M. & Kunisch, K., Feasible and non-interior path-following in constrained minimization with low multiplier regularity. *SIAM J. Control Optim.* **45** 4 (2006), 1198–1221. Zbl1121.49030 MR2257219
26. Hintermüller, M. & Kunisch, K., Path-following methods for a class of constrained minimization problems in function space. *SIAM J. Optim.* **17** (2006), 159–187. Zbl1137.49028 MR2219149

27. Hintermüller, M. & Laurain, A., A shape and topology optimization technique for solving a class of linear complementarity problems in function space. *Comput. Optim. Appl.* **46** 3 (2010), 535–569. Zbl1230.90187 MR2653723
28. Hintermüller, M. & Laurain, A., Optimal shape design subject to elliptic variational inequalities. *SIAM J. Control Optim.* **49** (2011), 1015–1047. Zbl1228.49045 MR2806573
29. Hintermüller, M., Mordukhovich, B. S. & Surowiec, T. M., Several approaches for the derivation of stationarity conditions for elliptic mpecs with upper-level control constraints. *Math. Program.* **146** (2014), 555–582. Zbl1332.90300 MR3232626
30. Hintermüller, M. & Ring, W., A level set approach for the solution of a state-constrained optimal control problem. *Numer. Math.* **98** (2004), 135–166. Zbl1059.65057 MR2076057
31. Hintermüller, M. & Wegner, D., Distributed optimal control of the Cahn–Hilliard system including the case of a double-obstacle homogeneous free energy density. *SIAM J. Control Optim.* **50** (2012), 388–418. Zbl1250.35131 MR2888271
32. Hintermüller, M. & Wegner, D., Optimal control of a semidiscrete Cahn–Hilliard–Navier-Stokes system. *SIAM J. Control Optim.* **52** (2014), 747–772. Zbl1293.49045 MR3170501
33. Hinze, M., Optimal and instantaneous control of the instationary Navier-Stokes equations, 1999. Habilitationsschrift.
34. Hinze, M. & Ziegenbalg, S., Optimal control of the free boundary in a two-phase Stefan problem. *J. Comput. Phys.* **223** (2007), 657–684. Zbl1115.80008 MR2319228
35. Hinze, M. & Ziegenbalg, S., Optimal control of the free boundary in a two-phase Stefan problem with flow driven by convection. *ZAMM Z. Angew. Math. Mech.* **87** (2007), 430–448. Zbl1123.49029 MR2333667
36. Kelley, C. T., *Iterative Methods for Optimization*, vol. 18 of *Frontiers in Applied Mathematics*. Society for Industrial and Applied Mathematics (SIAM), Philadelphia, PA, 1999. Zbl0934.90082 MR1678201
37. Kinderlehrer, D. & Stampacchia, G., *An Introduction to Variational Inequalities and Their Applications*, vol. 31 of *Classics in Applied Mathematics*. Society for Industrial and Applied Mathematics (SIAM), Philadelphia, PA, 2000. Reprint of the 1980 original.
38. Laurain, A. & Walker, S. W., Droplet footprint control. *SIAM J. Control Optim.* **53** 2 (2015), 771–799. Zbl1319.35310 MR3323539
39. Minty, G. J., On a "monotonicity" method for the solution of non-linear equations in Banach spaces. *Proc. Nat. Acad. Sci. U.S.A.* **50** (1963), 1038–1041. Zbl03200902 MR0162159
40. Moubachir, M. & Zolésio, J.-P., *Moving shape analysis and control*, vol. 277 of *Pure and Applied Mathematics (Boca Raton)*. Chapman & Hall/CRC, Boca Raton, FL, 2006. Applications to fluid structure interactions. Zbl1117.49003 MR2193461
41. Rockafellar, R. T., On the maximal monotonicity of subdifferential mappings. *Pacific J. Math.* **33** (1970), 209–216. Zbl0199.47101 MR0262827
42. Rockafellar, R. T., On the maximality of sums of nonlinear monotone operators. *Trans. Amer. Math. Soc.* **149** (1970), 75–88. Zbl0222.47017 MR0282272
43. Rockafellar, R. T., *Conjugate Duality and Optimization*. Society for Industrial and Applied Mathematics, Philadelphia, Pa., 1974. Lectures given at the Johns Hopkins University, Baltimore, Md., June, 1973, Conference Board of the Mathematical Sciences Regional Conference Series in Applied Mathematics, No. 16. Zbl0296.90036 MR0373611
44. Saguez, C., Optimal control of free boundary problems. In *System modelling and optimization (Budapest, 1985)*, vol. 84 of *Lecture Notes in Control and Inform. Sci.* Springer, Berlin, 1986, pp. 776–788. Zbl0599.49019 MR0903516
45. Satoh, W., Loughran, M. & Suzuki, H., Microfluidic transport based on direct electrowetting. *J. Appl. Phys.* **96** 1 (2004), 835–841.
46. Shapiro, B., Moon, H., Garrell, R. L. & Kim, C.-J., Equilibrium behavior of sessile drops under surface tension, applied external fields, and material variations. *J. Appl. Phys.* **93** 9 (2003), 5794–5811.

47. Walker, S. W., FELICITY: Finite Element Implementation and Computational Interface Tool for You. www.mathworks.com/matlabcentral/fileexchange/31141-felicity/.
48. Walker, S. W., Bonito, A. & Nochetto, R. H., Mixed finite element method for electrowetting on dielectric with contact line pinning. *Interfaces Free Bound.* **12** (2010), 85–119. Zbl1189.78056 MR2595379
49. Walker, S. W. & Shapiro, B., A control method for steering individual particles inside liquid droplets actuated by electrowetting. *Lab Chip* **5** (2005), 1404–1407.
50. Walker, S. W. & Shapiro, B., Modeling the fluid dynamics of electrowetting on dielectric (EWOD). *J. Microelectromech. S.* **15** (2006), 986–1000.
51. Walker, S. W., Shapiro, B. & Nochetto, R. H., Electrowetting with contact line pinning: Computational modeling and comparisons with experiments. *Physics of Fluids (1994–present)* **21** (2009), 102103.
52. Wheeler, A., Moon, H., Kim, C.-J., Loo, J. A. & Garrell, R. L., Electrowetting-based microfluidics for analysis of peptides and proteins by matrix-assisted laser desorption/ionization mass spectrometry. *Anal. Chem.* **76** (2004), 4833–4838.
53. Zeidler, E. *Nonlinear Functional Analysis and its Applications. II/B*. Springer-Verlag, New York, 1990. Nonlinear monotone operators, Translated from the German by the author and Leo F. Boron. Zbl0684.47029 MR1033498
54. Zeidler, E. *Applied Functional Analysis*, vol. 109 of *Applied Mathematical Sciences*. Springer-Verlag, New York, 1995. Main principles and their applications. Zbl0834.46003 MR1347692